



Published in final edited form as:

Pain. 2023 June 01; 164(6): 1340–1354. doi:10.1097/j.pain.0000000000002824.

Novel pro-resolving lipid mediator mimetic 3-oxa-PD1_{n-3} DPA reduces acute and chronic itch by modulating excitatory and inhibitory synaptic transmission and astroglial secretion of lipocalin-2 in mice

Kenta Furutani^{1,*}, Ouyang Chen^{1,2,*}, Aidan McGinnis¹, Yuqing Wang¹, Charles N Serhan³, Trond Vidar Hansen⁴, Ru-Rong Ji^{1,2,5}

¹Center for Translational Pain Medicine, Department of Anesthesiology, and Department of Neurobiology, Duke University Medical Center, Durham, NC 27710

²Department of Cell Biology, Duke University Medical Center, Durham, NC 27710

³Center for Experimental Therapeutics and Reperfusion Injury, Department of Anesthesiology, Perioperative and Pain Medicine, Hale Building for Transformative Medicine, Brigham and Women's Hospital and Harvard Medical School, Boston, Massachusetts, 02115

⁴Department of Pharmacy, Section for Pharmaceutical Chemistry, University of Oslo, PO Box 1068 Blindern, N-0316 Oslo, Norway

⁵Department of Neurobiology, Duke University Medical Center, Durham, NC 27710

Abstract

Specialized pro-resolving mediators (SPMs) have demonstrated potent analgesic actions in animal models of pathological pain. The actions of SPMs in acute and chronic itch are currently unknown. Recently, n-3 docosapentaenoic acid (DPA) was found to be a substrate for the biosynthesis of several novel families of SPMs; 3-oxa-PD1_{n-3} DPA (3-oxa-PD1) is an oxidation-resistant metabolic stable analogue of the n-3 DPA-derived protectin D1 (PD1). Herein, we demonstrate that 3-oxa-PD1 effectively reduces both acute and chronic itch in mouse models. Intrathecal injection of 3-oxa-PD1 (100 ng) reduced acute itch induced by either histamine, chloroquine, or morphine. Furthermore, intrathecal 3-oxa-PD1 effectively reduced chronic itch, induced by cutaneous T cell lymphoma (CTCL), allergic contact dermatitis with dinitrofluorobenzene, and psoriasis by imiquimod. Intratumoral injection of 3-oxa-PD1 also suppressed CTCL-induced chronic itch. Strikingly, this anti-pruritic effect lasted for several weeks after 1-week of intrathecal 3-oxa-PD1 treatment. Whole-cell recordings revealed significant increase in excitatory postsynaptic currents in spinal dorsal horn (SDH) neurons of CTCL mice,

Correspondence: Ru-Rong Ji, PhD, Departments of Anesthesiology and Neurobiology, Duke University Medical Center, Durham, North Carolina, 27710, Tel: 617-732-8852, ru-rong.ji@duke.edu.

*These authors contribute equally to this study.

Author contributions

K.F., O.C. and R.R.J developed the project; | T.V.H and C.N.S participated in project discussion; | K.F., O.C., A.M and Y.W. conducted experiments and analyzed data; | TVH provided 3-oxa-PD1. | K.F., O.C. and R.R.J. wrote the manuscript and other co-authors edited the manuscript.

Conflict of interest statement

The authors have no competing financial interest in this study.

but this increase was blocked by 3-oxa-PD1. 3-oxa-PD1 further increased inhibitory postsynaptic currents in SDH neurons of CTCL mice. CTCL increased the spinal levels of lipocalin-2 (LCN2), an itch mediator produced by astrocytes. 3-oxa-PD1 suppressed LCN2 production in CTCL mice and LCN2 secretion in astrocytes. Finally, CTCL-induced anxiety was alleviated by intrathecal 3-oxa-PD1. Our findings suggest that 3-oxa-PD1 potently inhibits acute and chronic itch via regulation of excitatory/inhibitory synaptic transmission and astroglial LCN2 production. Therefore, stable SPM analogs such as 3-oxa-PD1 could be useful to treat pruritus associated with different skin injuries.

Keywords

Cutaneous T cell lymphoma (CTCL); n-3 docosapentaenoic acid (n-3 DPA); excitatory postsynaptic currents (EPSCs); inhibitory postsynaptic currents (IPSC); 3-oxa-PD1_{n-3 DPA} (3-oxa-PD1); lipocalin-2 (LCN2); specialized proresolving mediators (SPMs); spinal cord dorsal horn (SDH)

1. Introduction

Many human skin diseases are associated with itch, and itch and pain are two distinct somatic sensations sharing similarities [1; 25; 40; 49]. Acute itch serves to protect the human body against harmful irritants [32], but chronic itch is operated by different mechanisms and share similar mechanisms with chronic pain [49; 94; 96]. As a result, chronic itch can significantly reduce quality of life, and scratching paradoxically exacerbates the itch sensation leading to a vicious cycle of 'itch-scratch-itch' [28; 30; 50]. Although antihistamines are commonly used to treat chronic pruritus, chronic pruritus can be histamine-independent refractory to conventional therapies [30; 95]. Despite current progress in treating inflammatory itch, chronic itch remains an area of considerable unmet need [22].

Recent studies have demonstrated that resolution of acute inflammation is an active process and requires the production of specialized pro-resolving mediators (SPMs), which are generated from omega-3 polyunsaturated fatty acids during the resolution phase of inflammation and play a critical role in the resolution physiology [18; 70]. SPMs are a rapidly expanding family of molecules that are derived from ω -3 eicosapentaenoic acid (EPA) and docosahexaenoic acid (DHA); they include the resolvins, protectins/neuroprotectins (e.g., PD1/NPD1) and maresins [18] (Fig. 1). Thanks to the elucidation of biosynthetic pathways of SPMs including protectins and their complete structures [5; 72], synthetic SPMs are now commercially available and have been tested in a wide range of animal models of human diseases. The synthetic SPMs exert strong protection against diseases in animal models of arthritis, infection, sepsis, and cancer, kidney injury, and Alzheimer's diseases/cognitive decline [18; 54; 78] and exhibit pro-resolving and anti-inflammatory properties [83]. In particular, synthetic SPMs have also been shown to potently reduce inflammatory, postoperative, and neuropathic pain [3; 35; 86; 87; 91; 92], as well as cancer pain [36; 93]. At this point, the potential roles of SPMs in acute and chronic itch are not known [33] and thus a goal of our present study.

Recently, n-3 docosapentaenoic acid (n-3 DPA) was found to be a substrate for the biosynthesis of several novel families of SPMs [27] (Fig. 1). One example is protectin D1_{n-3 DPA} (PD1_{n-3 DPA}), which exhibits potent anti-inflammatory and pro-resolving properties [6; 24; 27]. Recently, we reported the synthesis of a stable analogue of NPD1, 3-oxa-PD1_{n-3 DPA} (denoted 3-oxa-PD1), which could be resistant to β -oxidation (Fig. 1) [59]. Intriguingly, 3-oxa-PD1 not only reduced mechanical pain in a diabetic model but also suppressed itching behavior in a chronic itch model of cutaneous T cell lymphoma (CTCL) [59]. However, it is unclear whether 3-oxa-PD1 can control itch in different models with acute and persistent pruritus. The mechanisms by which 3-oxa-PD1 inhibits itch are also unknown. In this study, we demonstrated that 3-oxa-PD1 can effectively inhibit acute and chronic itch and further modulate excitatory and inhibitory neurotransmission in the spinal cord. Furthermore, 3-oxa-PD1 suppressed the production and secretion of LCN2, a prominent itch mediator produced by astrocytes [37; 73].

2. Materials and methods

2.1. Animals

C57BL/6J (stock No: 000664) and NOD.CB17-Prkdc^{scid} mice (stock No: 001303) were purchased from the Jackson Laboratory and maintained at Duke animal facility in a 12h light/dark cycle at 22 ± 1 °C with access to food and water ad libitum. All the animal procedures were approved by the Institutional Animal Care and Use Committees of Duke University.

2.2. Drugs and administration

3-oxa-PD1 was synthesized at the University of Oslo [59]. We purchased chloroquine (Cat. 1118000), 2,4-dinitrofluorobenzene (DNFB, Cat. 1118000), and histamine (Cat. H7250) from Sigma-Aldrich. PD1/NPD1 was from Cayman (Cat # 10010390), and morphine sulfate was from WEST-WARD pharmaceuticals. We injected the pruritic agents (histamine and chloroquine, 50 μ l) intradermally with a 28-Gauge needle in the nape (back of the neck). Morphine-induced itch was produced by intrathecal injection [88]. Intrathecal injection was performed by a lumbar puncture to deliver reagent into cerebrospinal fluid [29]. A valid spinal puncture was confirmed by a brisk tail-flick after the needle entry into subarachnoid space. Reagents were dissolved in PBS as vehicle if not specified. NPD1 and Oxa-PD1 were dissolved in ethanol and diluted in PBS. The final concentration was 5% ethanol for intrathecal and intratumor injection.

2.3. Acute and chronic itch models and behavioral analysis

Acute itch models.—Mice (C57BL/6J, 8–12 weeks old, of both sexes) were habituated to the testing environment daily for two days before analysis. The back of the neck of animals were shaved on the day before testing. The room temperature and humidity remained stable for all the experiments. Mice were put in plastic chambers (14 \times 18 \times 12 cm) on an elevated metal mesh floor and allowed 30 min for habituation. We intradermally injected 50 μ l of pruritic agents in the nape and video-recorded scratching behavior for 30 min in the absence of any observer. A scratch was counted when a mouse lifted its hind paw to scratch the shaved region and returned the paw to the floor or to the mouth for licking. Acute itch

was evoked by intradermal injection of 500 µg of histamine and 200 µg of chloroquine and intrathecal injection of 0.3 nmol of morphine [13; 88]. Spontaneous itch was video-recorded and assessed blindly.

Cutaneous T cell lymphoma (CTCL) model: Immune deficient mice (NOD.CB17-Prkdc^{scid}, 8 weeks old, both sexes) were used to produce xenograft model of CTCL as we previously described [26; 88]. CD4⁺ MyLa cell line was purchased from Sigma (Cat# 95051032) for mouse inoculation. MyLa cells were grown on RPMI medium (Gibco) with 10% human plasma and inclusion of IL-2 and IL-4 for 7 days. CTCL was generated via intradermal injection of CD4⁺ MyLa cells (1×10^7 cells in 100 µl) on the nape under 2% isoflurane anesthesia [26]. The scratching behavior was video recorded for 60 min using Sony HDR-CX610 camera. The video was subsequently played back offline and the number of scratches in every 60 min was counted blindly. We also measured tumor size by a digital caliper and calculated the volume using the equation: tumor volume = (short diameter)² × long diameter / 2.

DNFB-induced allergic contact dermatitis model.—Mice (C57BL/6J, 8–12 weeks old, both sexes) were used. We generated the allergic contact dermatitis model of chronic itch by applying the hapten DNFB onto the back skin as we previously described [47; 88]. DNFB was dissolved in a mixture of acetone:olive oil (4:1). The surface of the nape was shaved 1 day before sensitization. Mice were sensitized with 50 µL 0.5% DNFB solution by topical application to a 2 cm² area of shaved neck skin. 5 days later, mice were challenged with 30 µL 0.25% DNFB solution by painting the nape, then on day 5, 7, and 10. Spontaneous scratching behaviors were video-recorded on day 10 for 1 hour.

Imiquimod (IMQ)-induced psoriasis model.—C57BL/6J mice (8–12 weeks old, both sexes) were given daily topical application of 62.5 mg of 5% imiquimod on the shaved back skin for 4 consecutive days. The scratching behavior was video-recorded before (baseline) and after 3-oxa-PD1 treatment.

2.4. Spinal cord slice preparation and patch-clamp recordings in SDH neurons

As we previously reported [88], mice were anesthetized with urethane (1.5–2.0 g/kg, i.p.). After a dorsal laminectomy, the cervico-thoracic segment of the spinal cord was removed and placed into the pre-oxygenated, ice-cold cutting solution (in mM: sucrose 240, NaHCO₃ 25, KCl 2.5, NaH₂PO₄ 1.25, CaCl₂ 0.5, MgCl₂ 3.5). The mice were then immediately euthanized by decapitation. After removal of the arachnoid membrane, the cervical spinal cord was placed in an agar block and mounted on a metal stage. A transverse slice (300–400 µm thick) was cut on a vibrating microslicer (VT1200s, Leica, Wetzlar, Germany). Spinal cord slices were incubated for 30 min in artificial cerebrospinal fluid (ACSF) equilibrated with 95% O₂ and 5% CO₂ gas mixture. The ACSF contained (in mM): NaCl 126, KCl 3, CaCl₂ 2.5, MgCl₂ 1.3, NaH₂PO₄ 1.25, NaHCO₃ 26, and D-glucose 11. The spinal cord slice was placed in a recording chamber and perfused at a flow rate 2–4 ml/min with ACSF equilibrated with 95% O₂ and 5% CO₂ gas mixture and maintained at room temperature. Whole-cell patch-clamp recordings were made from outer lamina II (IIo) neurons with patch pipette electrodes having a resistance of 5–8 MΩ. Lamina II was identified as a translucent

band under a microscope (BX51WIF; Olympus) with light transmitted from below. All experiments were performed in voltage-clamp mode. The holding potential was set to -70 mV when recording of excitatory postsynaptic currents (EPSCs) and 0 mV when recording of inhibitory postsynaptic currents (IPSCs), respectively. The patch pipette solution for EPSC recording contained (in mM): Potassium gluconate 135, CaCl_2 0.5, MgCl_2 2, KCl 5, EGTA 5, HEPES 5, ATP-Mg salt 5, and the patch pipette solution for IPSC recording contained (in mM): CsSO_4 110, CaCl_2 0.5, MgCl_2 2, TEA 5, EGTA 5, HEPES 5, ATP-Mg salt 5. Drugs were dissolved in ASCF without alteration of the perfusion rate.

Signals were amplified using an Axopatch 700B amplifier (Molecular Devices, San Jose, CA) and were filtered at 2 kHz and digitized at 5 kHz. Data were collected and analyzed using pClamp 10.3 software (Molecular Devices, San Jose, CA). EPSCs and IPSCs were analyzed using Minianalysis ver. 6.0.3 (Synaptosoft, Decatur, GA). For data analysis, we collected EPSCs and IPSCs traces for 9 min, including 1-min baseline recordings, 3 min of drug perfusion (3-oxa-PD1), and 5 min washout. To quantify the impact of 3-oxa-PD1 on EPSCs and IPSCs, we analyzed the traces at 1 min (right before the drug perfusion) and at 5 min (1 min after the drug perfusion), as indicated in Fig. 6E, F and Fig. 7E, F. In all cases, n refers to the number of the neurons recorded, collected from 3–6 animals for each experimental condition. All drugs were bath applied to spinal cord slices by gravity perfusion via a three-way stopcock.

2.5. Primary culture of astrocytes

Cerebral cortex was isolated from neonatal CD1 mice (postnatal day 0, P0) of both sexes on ice. After digestion with trypsin for 6 min at 37°C , the brain tissues were filtered to collect brain cells. The brain cells were then seeded in culture flasks with DMEM medium (containing 10% fetal bovine serum) for 9 days. After vibration for 6–8 hours, astrocytes on the bottom of the flask were digested and seeded in six-well plates at the density of 8×10^5 /well with DMEM/F12 medium containing N2 supplement for 3 days before use.

2.6. Anxiety behavior

Anxiety behavior in chronic itch mice was assessed by open field test and elevated plus maze tests. Open field testing was performed in a $45 \times 45 \times 45$ cm³ square arena (TAP plastics) over 15 min. The center of the arena was defined as a center area that covered 50% of the total area. The total distance travelled, and time spent in the center area were automatically recorded and analyzed by ANY-maze (Stoelting Co.). The elevated plus maze apparatus (Stoelting Co.) is comprised of two open arms (35×5 cm²) and two closed arms ($35 \times 5 \times 15$ cm³) elevated 50 cm above the ground. Mice were placed in the center facing one of the two open arms and allowed to explore for 6 min. Anxiety-like behavior was assessed by time travelled within the open arms. The video and data were automatically recorded and analyzed by ANY-maze (Stoelting Co.).

2.7. ELISA

Three hours after intrathecal administration of Oxa-PD1 (100 ng/10 μL) or systemic injection (300 ng in 100 μL) in CTCL mice, mice were sacrificed by decapitation under isoflurane anesthesia. Then we collected cervical and lumbar spinal cord tissues. ELISA

kits for mouse lipocalin-2 were obtained from ThermoFisher (Cat # EMLCN2433707). The spinal cord tissues were homogenized in a lysis buffer containing protease and phosphatase inhibitors (RIPA buffer, sigma). For each ELISA assay, 50 µg of lysed spinal cord proteins or 50 µl of astrocyte culture medium were used. ELISA tests were conducted according to the manufacturer's instructions. The standard curve was included in each experiment.

2.8. Statistical analysis

GraphPad Prism 7.0 (GraphPad, San Diego, CA) was used for statistical analysis, and all data were expressed as mean ± s.e.m, as indicated in the figure legends. Electrophysiological data were analyzed using paired or unpaired two-tailed Student's t-test and 2-sample Kolmogorov-Smirnov test. Behavioral data were analyzed using Student's t-test (two groups) or two-way ANOVA followed by post-hoc Tukey's test or Bonferroni test. The criterion for statistical significance was $P < 0.05$.

3. Results

3.1. Intrathecal injection of 3-oxa-PD1 reduces acute itch

3-oxa-PD1 is a novel SPM mimetic, derived from n-3 DPA (Fig. 1). First, we tested the anti-pruritic actions of 3-oxa-PD1 in acute itch models. Acute itch can be characterized as histaminergic or nonhistaminergic itch. Histamine elicits acute itch via activation of histamine receptors and TRPV1 [31], whereas chloroquine (CQ), an anti-malaria drug can elicit histamine-independent itch via activation of MrgprA3 receptors and TRPA1 [45; 89]. Intradermal administration of histamine and CQ evoked robust acute itch, as indicated by increased scratching bouts in 30 min (Fig. 2A–D). Notably, intrathecal (i.t.) administration of 3-oxa-PD1 (100 ng) prevented acute itch, induced by histamine ($P < 0.0001$, Fig. 2B) and CQ ($P < 0.0001$, Fig. 2D). Intrathecal administration of morphine is also known to produce pruritus in mice by acting on inhibitory neurons and gastrin-releasing peptide receptor (GRPR) [52; 60; 88]. We found i.t. administration of 0.3 nmol of morphine induced robust scratching for 20 min (Fig. 2E). The morphine-induced pruritus was completely blocked by the i.t. treatment of 3-oxa-PD1 ($P < 0.001$, Fig. 2F). Together, these results indicate that 3-oxa-PD1 is highly effective in suppressing acute itch in different animal models.

3.2. Intrathecal 3-oxa-PD1 produces greater inhibition of chronic itch than PD1 in CTCL mice

In our earlier report, we demonstrated that i.t. administration of PD1 or 3-oxa-PD1 reduced chronic itch in a cancer model of CTCL [59]. We further compared the efficacy of PD1 and 3-oxa-PD1 in this model. Following i.t. administration, both PD1 (100 ng) and 3-oxa-PD1 (100 ng) produced significant reductions of scratches at 1 hour ($P < 0.0001$ vs. vehicle), 3 hours ($P < 0.0001$ vs. vehicle), and 5 hours ($P < 0.0001$ vs. vehicle), but the anti-pruritic effects of both agents recovered 24 hours after the administration (Fig. 3A). However, 3-oxa-PD1 produced greater itch reduction at 3 hours ($P < 0.01$) and 5 hours ($P < 0.01$) than PD1 (Fig. 3A). Rotarod testing in both naïve and CTCL animals showed no sign of motor impairment following i.t. 3-oxa-PD1 treatment; and 3-oxa-PD1 slightly increased the fall latency (Fig. 3B). These results suggest that the 3-oxa-PD1 is more effective than PD1 for

the control of chronic itch, most likely due to increased metabolic stability of 3-oxa-PD1 [59].

3.3. Sustained 3-oxa-PD1 treatment results in long-lasting inhibition of chronic itch in CTCL mice

Next, we examined whether repeated injections of 3-oxa-PD1 would cause antipruritic tolerance or accumulating benefits. To this end, we treated CTCL animals with daily i.t. injections of Oxa-PD1 for 7 days and assessed itch behavior at 1 day and 25 days after the treatment/last injection (Fig. 4A). Surprisingly, we observed profound inhibition of itch not only at 1 day after the treatment ($P < 0.0001$ vs. vehicle, Fig. 4B) but also at 25 days after the treatment (CTCL Day 55, $P < 0.0001$ vs. vehicle, Fig. 4C). Thus, repeated i.t. injections of 3-oxa-PD1 do not cause antipruritic tolerance. Instead, we observed accumulating and sustained anti-itch effect of the treatment, even 3 weeks after the last injection. Furthermore, we found this treatment did not affect the tumor growth on CTCL Day 30 ($P > 0.05$ vs. vehicle, Fig. 4D) and CTCL Day 55 ($P > 0.05$, Fig. 4E). Therefore, the antipruritic action of i.t. 3-oxa-PD1 is not a result of tumor suppression.

3.4. Intratumoral injection of 3-oxa-PD1 reduces chronic itch in CTCL mice

Our data suggest that 3-oxa-PD1 can effectively control acute and chronic itch via spinal action. Next, we investigated whether 3-oxa-PD1 could control itch via local and peripheral actions. To this end, we conducted intra-tumor administration of 3-oxa-PD1 (100 ng) via a single injection (20 μ L) into the skin lymphoma on CTCL Day 35 (Fig. 5A,B). Intratumoral 3-oxa-PD1 significantly reduced the CTCL-induced pruritus at 1 hour ($P < 0.0001$, vs. vehicle, Fig. 5B) and 3 hours ($P < 0.0001$, vs. vehicle, Fig. 5B). Intra-tumor 3-oxa-PD1 (100 ng) on CTCL Day 55 also significantly reduced pruritus at 1 hour ($P < 0.05$, vs. vehicle, Fig. 5C). These results suggest that 3-oxa-PD1 may also reduce chronic itch via peripheral modulation.

3.5. 3-oxa-PD1 modulates excitatory and inhibitory spinal transmission in cervical spinal cord neurons in CTCL mice

Spinal cord synaptic plasticity manifests as central sensitization and plays an important role in chronic itch sensitization [1; 34]. To determine the synaptic mechanisms by which CTCL modulates chronic itch, we conducted patch-clamp recordings in spinal cord slices to measure spontaneous excitatory postsynaptic currents (sEPSCs, Fig. 6) and spontaneous inhibitory postsynaptic currents (sIPSCs, Fig. 7) in lamina IIo interneurons. These interneurons are known to form a microcircuit with input from C-fiber afferents and output to lamina I projection neurons, contributing to itch processing [10; 80].

We first tested the effects of 3-oxa-PD1 on sEPSCs in spinal cord slices prepared from naïve mice (CB17 background) and CTCL mice (Fig. 6A–J). Compared with naïve animals, the baseline frequencies of sEPSCs were significantly higher in CTCL mice ($P = 0.0002$, Fig. 6C), whereas the baseline amplitudes of sEPSCs did not change ($P = 0.91$, Fig. 6D). In spinal cord slices from naïve mice, bath application of 3-oxa-PD1 (10 ng/ml) did not affect the sEPSC frequencies (2.7 ± 0.5 Hz vs. 3.7 ± 0.9 Hz, before and after application, $n = 13$, $P = 0.21$, paired t-test) and sEPSC amplitudes (10.6 ± 1.1 pA vs. 9.6 ± 0.6 pA, $n = 13$

neurons, $P = 0.19$, paired t-test). Time course analysis of sEPSCs revealed that superfusion of spinal cord slices from CTCL mice with 3-oxa-PD1 (10 ng/ml, 3 min) produced a rapid but transient inhibition of sEPSC frequency (Fig. 6E). Only a mild inhibition in sEPSC amplitude was observed by this treatment (Fig. 6F). The inhibitory effect of 3-oxa-PD1 was washed out in 5 min (Fig. 6E). 3-oxa-PD1 (10 ng/ml) significantly reduced sEPSC frequency 4 min after the perfusion ($P = 0.008$, Fig. 6G), which was also revealed by cumulative probability of sEPSCs ($P < 0.001$, Fig. 6H). At the same time point, 3-oxa-PD1 (10 ng/ml) produced a mild but significant inhibition of sEPSCs amplitude (9.7 ± 0.5 vs. 8.9 ± 0.5 pA, before and after the treatment, $n = 14$, $P = 0.037$, paired t-test, Fig. 6I, J).

Next, we investigated the effects of 3-oxa-PD1 on sIPSCs in cervical spinal cord slices from naïve and CTCL mice (Figure 7A–J). The baseline frequencies and amplitudes of sIPSCs were not significantly different between CTCL and naïve groups (Figure 7A–D). In spinal cord slides of naïve mice, bath application of 3-oxa-PD1 (10 ng/ml) slightly increased sIPSCs but had no significant impact on the sIPSC frequencies (1.6 ± 0.5 Hz vs. 2.6 ± 0.5 Hz, before and after application, respectively, $n=10$, $P = 0.14$, paired t-test) and sIPSC amplitudes (12.2 ± 0.7 pA vs. 16.3 ± 2.8 pA, respectively, $n=10$, $P=0.16$, paired t-test). Time course analysis of sIPSCs demonstrate that superfusion of spinal cord slices from CTCL mice with 3-oxa-PD1 (10 ng/ml, 3 min) produced a rapid but transient increase of sIPSC frequency (Fig. 7E). Only a very brief increase in sIPSC amplitude was observed by this treatment (Fig. 7F). The facilitatory effect of 3-oxa-PD1 was washed out in 5 min (Fig. 7E). Of interest, in spinal cord slices from CTCL mice, 3-oxa-PD1 (10 ng/mL) significantly increased the sIPSC frequency (Fig. 7G), at 4 min after the perfusion (Fig. 7E), which was also revealed by cumulative probability of sIPSCs ($P < 0.05$, Fig. 7H). This treatment had no significant impact on sIPSC amplitudes (12.0 ± 1.4 pA vs. 18.1 ± 5.0 pA, respectively, $n = 13$, $P = 0.17$, paired t-test, Fig. 7I, J).

Collectively, these findings from sEPSC and sIPSC recordings indicate that 3-oxa-PD1 can regulate both excitatory and inhibitory synaptic transmission by decreasing sEPSCs and increasing sIPSCs. Notably, the percentage change in sIPSCs appeared to be greater than that of sEPSCs (Fig. 6E,7E). The opposite modulation of both EPSC and IPSC will lead to a strong suppression of central sensitization underlying the genesis of persistent itch.

3.6. 3-oxa-PD1 reduces persistent itch in contact dermatitis and psoriasis models

Allergic contact dermatitis (ACD) is a common cause of chronic itch [41; 75]. We induced ACD by DNFB treatment and tested the anti-itch effect of Oxa-PD1 on Day 10 (Fig. 8A). DNFB elicited marked and persistent itch on day 10 (Fig. 8B). Intrathecal injection of 3-oxa-PD1 (100 ng) significantly reduced the DNFB-evoked itching behaviors at 1 hour ($P < 0.05$ vs. vehicle) and 3 hours ($P < 0.05$ vs. vehicle) but not at 5 and 24 hours (Fig. 8B). Imiquimod (IMQ) is an agonist of Toll-like receptor 7 and an approved anti-cancer treatment. Topic application of IMQ elicited strong pruritus [51]. Repeated IMQ treatment (Fig. 8C) has been shown to induce psoriasis and persistent itch [84]. Intrathecal injection of 3-oxa-PD1 (100 ng) significantly reduced the IMQ-evoked pruritus at 1, 3, and 5 hours ($P < 0.05$ vs. vehicle, Fig. 8D). These results further suggest that 3-oxa-PD1 can exert antipruritic action in clinically relevant persistent itch conditions.

3.7. 3-oxa-PD1 inhibits the spinal production of LCN2 in CTCL mice and astrocyte release of LCN2

LCN2 is an innate immune factor and can be secreted by activated immune cells and astrocytes. STAT3-dependent upregulation of LCN2 was shown to be crucial for inducing chronic itch [73]. To elucidate the mechanism by which 3-oxa-PD1 exerts antipruritic actions, we collected cervical and lumbar spinal cord segments from CTCL mice and supernatant of cultured astrocytes to measure LCN2 levels in vivo (Fig. 9A–D) and in vitro (Fig. 9E,F) by ELISA. For in vivo analysis, we collected spinal cord segments at 3 hours after intrathecal injection (100 ng, Fig. 9A) or intraperitoneal injection (i.p., 300 ng, Fig. 9C) of 3-oxa-PD1 or vehicle. We found that i.t. treatment of 3-oxa-PD1 significantly reduced the LCN2 levels in both cervical spinal segments ($P = 0.0015$) and lumbar spinal cord segments ($P = 0.0025$) of CTCL mice (Fig. 9B). We also observed that LCN2 levels were very low in naïve animals but dramatically increased in CTCL animals ($P < 0.0001$, Fig. 9D). Furthermore, i.p. treatment of 3-oxa-PD1 significantly reduced the LCN2 levels in both cervical spinal cord segments ($P < 0.0001$) and lumbar spinal cord segments ($P < 0.0001$) of CTCL mice (Fig. 9D). To determine the involvement of astrocytes in secreting LCN2, we prepared primary cultures of astrocytes from mouse cortices (Fig. 9E). We detected high basal levels of LCN2 in culture medium of astrocyte cultures (Fig. 9F). 3-oxa-PD1 treatment (100 ng/ml, 24 h) significantly decreased LCN2 secretion ($P = 0.0022$, Fig. 9F). Lipopolysaccharide (LPS, 100 ng/ml, 24 h) failed to increase LCN2 secretion in astrocyte cultures, but 3-oxa-PD1 still significantly decreased LCN2 secretion ($P < 0.01$, Fig. 9F). Collectively, these results suggest that 1) 3-oxa-PD1 can suppress both in vivo production and in vitro secretion of LCN2 and 2) 3-oxa-PD1 may inhibit chronic itch by inhibiting LCN2 signaling in the spinal cord.

3.8. 3-oxa-PD1 alleviates chronic itch-induced anxiety

Chronic itch conditions are associated with higher rates of stress, anxiety, depression, leading to an impairment of quality of life [68]. In patients with plaque psoriasis and atopic dermatitis, severe pruritus is associated with higher anxiety and depression scores [21; 58]. Therefore, we examined anxiety-related behavior on naïve and CTCL mice using open-field and elevated plus maze tests (Fig. 10A–D). In open-field testing, we observed that the inner zone stay duration ($P < 0.0001$, Fig. 10B) and travel distance ($P = 0.027$, Fig. 10B) were significantly shorter in CTCL mice compared to naïve mice, although the total travel distance did not differ between these two groups (Fig. 10A–B). Furthermore, elevated plus maze testing revealed that CTCL mice showed significantly shorter open arm stay duration ($P = 0.0091$, Fig. 10D) and open arm travel distance ($P = 0.020$, Fig. 10D), although the total travel distance did not differ between these two groups (Fig. 10D). Next, we tested the effects of 3-oxa-PD1 on these anxiety-related behaviors in CTCL mice (Fig. 10E). Notably, i.t. administration of 3-oxa-PD1 (100 ng) significantly improved the anxiety-related behaviors in open-field testing (Fig. 10F,G) and elevated plus maze testing (Fig. 10H,I). Together, these results suggest that 1) CTCL-induced chronic itch is associated with anxiety and 2) 3-oxa-PD1 can further alleviate chronic itch-induced anxiety.

4. Discussion

In the present report, we demonstrate the antipruritic efficacy of a new SPM mimetic 3-oxa-PD1 in several itch models; Namely 1) histamine-induced acute itch, 2) chloroquine-induced histamine-independent itch, 3) intrathecal morphine-induced central itch, 4) allergic contact dermatitis-induced persistent itch by DNFB, 5) psoriasis-induced persistent itch IMQ, and 6) the CTCL-induced chronic cancer itch. Moreover, we found that both central and peripheral routes of 3-oxa-PD1 delivery are effective in itch suppression. Especially, the anti-itch effect can last for several weeks after one-week intrathecal treatment of 3-oxa-PD1 in the cancer itch model. Mechanistically, we demonstrated that spinal perfusion of 3-oxa-PD1 (10 ng/ml, ~1 nM) drastically enhanced inhibitory synaptic transmissions in SDH neurons from mice with chronic itch. Furthermore, we showed that anxiety is a comorbidity of lymphoma-induced chronic itch and 3-oxa-PD1 significantly improved the anxiety-related behaviors in CTCL mice. These results indicate that 3-oxa-PD1 is a novel and potent antipruritic treatment.

Increasing evidence suggests that SPMs possess potent analgesic actions in animal models of inflammatory, postoperative, neuropathic, and cancer pain via immune, glial, and neuronal modulation (reviewed in [33; 35]). Pain and itch are different sensory modalities: pain suppresses itch, whereas analgesics such as morphine can elicit itch [15; 19; 41]. On the other hand, inflammation induces both pain and itch [50]. TRP channels, such as TRPA1, TRPV1, TRPV4, and TRPC3 are required for the induction of both pain and itch [8; 14; 20; 53; 55; 57; 63; 90]. Limited studies have shown that SPMs alleviate itch by peripheral mechanisms, such as reducing skin inflammation and modulation of TRP channels. Resolvin E1 attenuates murine psoriatic dermatitis, a chronic itch disease, by inhibiting migration of cutaneous dendritic cells and $\gamma\delta$ T cells [69]. Systemic resolvin D3 treatment was shown to prevent the development of psoriasiform itch and skin inflammation and further inhibit the TRPV1 function in cultured sensory neurons [43]. Our previous study demonstrated that a single intrathecal injection of PD1 and/or 3-oxa-PD1_{n-3} DPA reduced CTCL-induced chronic itch for several hours [59]. In the present study, we further revealed that 3-oxa-PD1 elicited more potent anti-itch actions than PD1, due to a possible increase in lipid stability mediated by β -oxidation (Fig. 1) [59].

Our findings highlight a central modulation of chronic itch by intrathecal 3-oxa-PD1. Central sensitization underlies acute and chronic itch [2; 50]. It can manifest as increased excitatory synaptic transmission in the spinal cord itch circuitry [11; 34], which could be mediated by GRPR⁺ excitatory neurons. Both GRP and GRPR-expressing neurons are critically involved in chronic itch [76; 77]. In chronic itch, GRP-GRPR signaling is enhanced [37; 74]. Consistently, we obtained significant increases in excitatory synaptic transmission (sEPSC) in SDH neurons following CTCL-induced chronic itch, as result of presynaptic modulation. Central sensitization is also characterized by loss of inhibition (disinhibition) in both chronic pain and itch conditions [42; 50]. Spinal cord disinhibition is sufficient to drive chronic pruritus [9; 66]. Recent studies revealed that intrathecal opioid-induced itch is also mediated disinhibition in the spinal cord [60; 88]. Indeed, activation of GABAergic and glycinergic transmission effectively inhibited pruritus [11; 23; 44; 65]. Although we only saw a tendency of IPSC reduction in SDH neurons after chronic itch, we

found that 3-oxa-PD1 perfusion caused rapid and profound increases in sIPSCs. Therefore, it is conceivable that intrathecal 3-oxa-PD1 can suppress chronic itch and opioid-induced itch by increasing IPSCs, therefore counteracting disinhibition in the spinal circuit of itch.

Emerging evidence suggests that spinal glial cells play an important role in driving chronic itch [34; 82]. Intrathecal injection of astrocyte inhibitor alpha amino adipate did not alter acute itch but reduced dry skin-induced chronic itch [47]. Chronic itch is associated with persistent astrogliosis, as well as upregulations of toll-like receptor 4 (TLR4) and the transcription factor STAT3 in spinal cord astrocytes [48; 73; 81]. Genetic deletion of *Tlr4* or *Stat3* or pharmacological inhibition of TLR4 in SDH reduced astrogliosis and pruritus in mouse dry skin and DNFB models [47; 73]. Interestingly, lipocalin-2 (LCN2), also known as neutrophil gelatinase-associated lipocalin, is enriched in reactive astrocytes and contributes to neurodegeneration [46; 85]. STAT3-induced upregulation of LCN2 plays a crucial role in chronic itch. LCN2 was upregulated in reactive astrocytes in chronic itch and sufficient to enhance GPR-evoked pruritus [74]. Furthermore, GRP-induced excitability of GRPR⁺ SDH neurons is enhanced by LCN2 released from reactive astrocytes [37]. Our ELISA analysis revealed that 3-oxa-PD1 reduced LCN2 levels in the spinal cord of CTCL mice and suppressed LCN2 secretion in astrocyte cultures. It is likely that 3-oxa-PD1 may inhibit itching via astroglial signaling.

There are also limitations of this study. The receptor of 3-oxa-PD1 remains to be identified. It is generally believed that the biological actions of SPMs are mediated by specific G-protein coupled receptors (GPCRs), such as GPR32 for RvD1, GPR18 for RvD2, ChemR23 for RvE1, GPR37 for PD1/NPD1, and LGR6 for MaR1 [4; 7; 16; 17; 39]. SPMs modulate the activities of TRP channels (e.g., TRPA1 and TRPV1) via GPCR signaling [43; 61; 62; 71]. It is also possible that SPMs at high concentrations, may directly interact with ion channels. Mas-related GPCRs such as MrgprA3 was identified as an itch receptor in mice [45] and MRGPRX4 was proposed as a human itch receptor [12; 56; 97]. It will be of considerable interest to study interactions of 3-oxa-PD1 with different types of itch receptors. Another limitation of this study is the cellular targets of 3-oxa-PD1 are still elusive. Oxa-PD1 may act on multiple cell types, including neurons and glial cells. Further studies are needed to explore these cellular mechanisms of 3-oxa-PD1 using *in vitro* systems.

In conclusion, our results indicate that the new 3-oxa-PD1, a metabolically stable analog of PD1/NPD1 [59], can potently inhibit acute and chronic itch in various mouse models. Mechanistically, 3-oxa-PD1 may inhibit itch via modulation of both excitatory and inhibitory synaptic transmission and regulation of astrocyte signaling (Fig. 11). Chronic itch remains a major health concern in skin diseases such as atopic dermatitis, contact dermatitis, allergic contact dermatitis and xerosis [94]. It also occurs in systemic diseases such as cholestatic liver diseases, kidney diseases (e.g., uremia), and diabetes [14; 38]. Notably, antihistamines do not work for most chronic itch conditions [79]. Advances in our understanding of the neuroimmunology of chronic itch have led to the clinical applications of type 2 cytokine blockers (e.g., IL-4, IL-13, IL-31, and IL-33 blockers) for the treatment of atopic dermatitis [22]. Even if these agents are effective, the appearance of side effects such as drowsiness, nausea, constipation, and infection, can be a problem in the

treatment of pruritus. In particular, CTCLs are the most frequent primary skin lymphomas and cause intractable pruritus in advanced stages [64; 67]. SPMs promote the resolution of inflammation and diseases via immune, glial, and neuronal modulations and also have shown no obvious side effects in animal studies and/or human trials [33]. However, as lipid mediators, SPMs are limited by their local pharmacokinetics. Thus, metabolically stable analogs of SPMs, such as the 3-oxa-PD1, may be promising as highly effective anti-pruritic agents. Especially, the antipruritic action could be achieved by intra-tumoral injection in cancer patients with severe itch.

Acknowledgments

We thank Dr. Jannicke I. Nesman for preparing 3-Oxa-PD1_{n-3} DPA. This study was supported by Duke University Anesthesiology Research Funds, NIH R01 grant DE17794, and DoD grant W81XWH2110885 to R.-R.Ji. C.N.S is supported by NIH R-35GM139430 (CNS) and T.V.H was supported by The Norwegian Research Council (FRIPRO-FRINATEK 230470).

References

- [1]. Akiyama T, Carstens E. Neural processing of itch. *Neuroscience* 2013;250:697–714. [PubMed: 23891755]
- [2]. Akiyama T, Carstens MI, Carstens E. Enhanced responses of lumbar superficial dorsal horn neurons to intradermal PAR-2 agonist but not histamine in a mouse hindpaw dry skin itch model. *J Neurophysiol* 2011;105(6):2811–2817. [PubMed: 21430273]
- [3]. Allen BL, Montague-Cardoso K, Simeoli R, Colas RA, Oggero S, Vilar B, McNaughton PA, Dalli J, Perretti M, Sher E, Malcangio M. Imbalance of pro-resolving lipid mediators in persistent allodynia dissociated from signs of clinical arthritis. *Pain* 2020.
- [4]. Arita M, Ohira T, Sun YP, Elangovan S, Chiang N, Serhan CN. Resolvin E1 selectively interacts with leukotriene B4 receptor BLT1 and ChemR23 to regulate inflammation. *J Immunol* 2007;178(6):3912–3917. [PubMed: 17339491]
- [5]. Aursnes M, Tungen JE, Colas RA, Vlasakov I, Dalli J, Serhan CN, Hansen TV. Synthesis of the 16S,17S-Epoxyprotectin Intermediate in the Biosynthesis of Protectins by Human Macrophages. *J Nat Prod* 2015;78(12):2924–2931. [PubMed: 26580578]
- [6]. Aursnes M, Tungen JE, Vik A, Colas R, Cheng CY, Dalli J, Serhan CN, Hansen TV. Total synthesis of the lipid mediator PD1_{n-3} DPA: configurational assignments and anti-inflammatory and pro-resolving actions. *J Nat Prod* 2014;77(4):910–916. [PubMed: 24576195]
- [7]. Bang S, Xie YK, Zhang ZJ, Wang Z, Xu ZZ, Ji RR. GPR37 regulates macrophage phagocytosis and resolution of inflammatory pain. *J Clin Invest* 2018;128(8):3568–3582. [PubMed: 30010619]
- [8]. Bautista DM, Jordt SE, Nikai T, Tsuruda PR, Read AJ, Poblete J, Yamoah EN, Basbaum AI, Julius D. TRPA1 mediates the inflammatory actions of environmental irritants and proalgesic agents. *Cell* 2006;124(6):1269–1282. [PubMed: 16564016]
- [9]. Bourane S, Duan B, Koch SC, Dalet A, Britz O, Garcia-Campmany L, Kim E, Cheng L, Ghosh A, Ma Q, Goulding M. Gate control of mechanical itch by a subpopulation of spinal cord interneurons. *Science* 2015;350(6260):550–554. [PubMed: 26516282]
- [10]. Braz J, Solorzano C, Wang X, Basbaum AI. Transmitting Pain and Itch Messages: A Contemporary View of the Spinal Cord Circuits that Generate Gate Control. *Neuron* 2014;82(3):522–536. [PubMed: 24811377]
- [11]. Braz JM, Juarez-Salinas D, Ross SE, Basbaum AI. Transplant restoration of spinal cord inhibitory controls ameliorates neuropathic itch. *J Clin Invest* 2014;124(8):3612–3616.
- [12]. Cao C, Kang HJ, Singh I, Chen H, Zhang C, Ye W, Hayes BW, Liu J, Gumpfer RH, Bender BJ, Slocum ST, Krumm BE, Lansu K, McCorvy JD, Kroeze WK, English JG, DiBerto JF, Olsen RHJ, Huang XP, Zhang S, Liu Y, Kim K, Karpiak J, Jan LY, Abraham SN, Jin J, Shoichet BK, Fay JF, Roth BL. Structure, function and pharmacology of human itch GPCRs. *Nature* 2021;600(7887):170–175. [PubMed: 34789874]

- [13]. Chandra S, Wang Z, Tao X, Chen O, Luo X, Ji RR, Bortsov AV. Computer-aided Discovery of a New Nav1.7 Inhibitor for Treatment of Pain and Itch. *Anesthesiology* 2020;133(3):611–627. [PubMed: 32788559]
- [14]. Chen Y, Wang ZL, Yeo M, Zhang QJ, Lopez-Romero AE, Ding HP, Zhang X, Zeng Q, Morales-Lazaro SL, Moore C, Jin YA, Yang HH, Morstein J, Bortsov A, Krawczyk M, Lammert F, Abdelmalek M, Diehl AM, Milkiewicz P, Kremer AE, Zhang JY, Nackley A, Reeves TE, Ko MC, Ji RR, Rosenbaum T, Liedtke W. Epithelia-Sensory Neuron Cross Talk Underlies Cholestatic Itch Induced by Lysophosphatidylcholine. *Gastroenterology* 2021.
- [15]. Chen ZF. A neuropeptide code for itch. *Nat Rev Neurosci* 2021;22(12):758–776. [PubMed: 34663954]
- [16]. Chiang N, Dalli J, Colas RA, Serhan CN. Identification of resolvin D2 receptor mediating resolution of infections and organ protection. *J Exp Med* 2015;212(8):1203–1217. [PubMed: 26195725]
- [17]. Chiang N, Libreros S, Norris PC, de la Rosa X, Serhan CN. Maresin 1 activates LGR6 receptor promoting phagocyte immunoresolvent functions. *J Clin Invest* 2019;129(12):5294–5311. [PubMed: 31657786]
- [18]. Chiang N, Serhan CN. Specialized pro-resolving mediator network: an update on production and actions. *Essays Biochem* 2020;64(3):443–462. [PubMed: 32885825]
- [19]. Dong X, Dong X. Peripheral and Central Mechanisms of Itch. *Neuron* 2018;98(3):482–494. [PubMed: 29723501]
- [20]. Donnelly CR, Chen O, Ji RR. How Do Sensory Neurons Sense Danger Signals? *Trends Neurosci* 2020;43(10):822–838. [PubMed: 32839001]
- [21]. Eckert L, Gupta S, Amand C, Gadkari A, Mahajan P, Gelfand JM. Impact of atopic dermatitis on health-related quality of life and productivity in adults in the United States: An analysis using the National Health and Wellness Survey. *J Am Acad Dermatol* 2017;77(2):274–279 e273. [PubMed: 28606711]
- [22]. Erickson S, Heul AV, Kim BS. New and emerging treatments for inflammatory itch. *Ann Allergy Asthma Immunol* 2021;126(1):13–20. [PubMed: 32497711]
- [23]. Foster E, Wildner H, Tudeau L, Haueter S, Ralvenius WT, Jegen M, Johannssen H, Hosli L, Haenraets K, Ghanem A, Conzelmann KK, Bosl M, Zeilhofer HU. Targeted ablation, silencing, and activation establish glycinergic dorsal horn neurons as key components of a spinal gate for pain and itch. *Neuron* 2015;85(6):1289–1304. [PubMed: 25789756]
- [24]. Gobbetti T, Dalli J, Colas RA, Federici Canova D, Aursnes M, Bonnet D, Alric L, Vergnolle N, Deraison C, Hansen TV, Serhan CN, Perretti M. Protectin D1n-3 DPA and resolvin D5n-3 DPA are effectors of intestinal protection. *Proc Natl Acad Sci U S A* 2017;114(15):3963–3968. [PubMed: 28356517]
- [25]. Han L, Dong X. Itch mechanisms and circuits. *Annu Rev Biophys* 2014;43:331–355. [PubMed: 24819620]
- [26]. Han Q, Liu D, Convertino M, Wang Z, Jiang C, Kim YH, Luo X, Zhang X, Nackley A, Dokholyan NV, Ji RR. miRNA-711 Binds and Activates TRPA1 Extracellularly to Evoke Acute and Chronic Pruritus. *Neuron* 2018;99(3):449–463 e446. [PubMed: 30033153]
- [27]. Hansen TV, Dalli J, Serhan CN. The novel lipid mediator PD1n-3 DPA: An overview of the structural elucidation, synthesis, biosynthesis and bioactions. *Prostaglandins Other Lipid Mediat* 2017;133:103–110. [PubMed: 28602942]
- [28]. Hay RJ, Johns NE, Williams HC, Bolliger IW, Dellavalle RP, Margolis DJ, Marks R, Naldi L, Weinstock MA, Wulf SK, Michaud C, C JLM, Naghavi M. The global burden of skin disease in 2010: an analysis of the prevalence and impact of skin conditions. *J Invest Dermatol* 2014;134(6):1527–1534. [PubMed: 24166134]
- [29]. Hylden JL, Wilcox GL. Intrathecal morphine in mice: a new technique. *Eur J Pharmacol* 1980;67(2–3):313–316.
- [30]. Ikoma A, Steinhoff M, Stander S, Yosipovitch G, Schmelz M. The neurobiology of itch. *Nat Rev Neurosci* 2006;7(7):535–547.

- [31]. Imamachi N, Park GH, Lee H, Anderson DJ, Simon MI, Basbaum AI, Han SK. TRPV1-expressing primary afferents generate behavioral responses to pruritogens via multiple mechanisms. *Proc Natl Acad Sci USA* 2009;106(27):11330–11335.
- [32]. Jeffry J, Kim S, Chen ZF. Itch signaling in the nervous system. *Physiology (Bethesda)* 2011;26(4):286–292. [PubMed: 21841076]
- [33]. Ji RR. Specialized Pro-Resolving Mediators as Resolution Pharmacology for the Control of Pain and Itch Annual Review of Pharmacology and Toxicology 2022;In press.
- [34]. Ji RR, Donnelly CR, Nedergaard M. Astrocytes in chronic pain and itch. *Nat Rev Neurosci* 2019.
- [35]. Ji RR, Xu ZZ, Strichartz G, Serhan CN. Emerging roles of resolvins in the resolution of inflammation and pain. *Trends Neurosci* 2011.
- [36]. Khasabova IA, Golovko MY, Golovko SA, Simone DA, Khasabov SG. Intrathecal Administration of Resolvin D1 and E1 Decreases Hyperalgesia in Mice with Bone Cancer Pain: Involvement of Endocannabinoid Signaling. *Prostaglandins Other Lipid Mediat* 2020:106479. [PubMed: 32745525]
- [37]. Koga K, Yamagata R, Kohno K, Yamane T, Shiratori-Hayashi M, Kohro Y, Tozaki-Saitoh H, Tsuda M. Sensitization of spinal itch transmission neurons in a mouse model of chronic itch requires an astrocytic factor. *J Allergy Clin Immunol* 2020;145(1):183–191 e110. [PubMed: 31787267]
- [38]. Kremer AE, Feramisco J, Reeh PW, Beuers U, Oude Elferink RP. Receptors, cells and circuits involved in pruritus of systemic disorders. *Biochim Biophys Acta* 2014;1842(7):869–892. [PubMed: 24568861]
- [39]. Krishnamoorthy S, Recchiuti A, Chiang N, Yacoubian S, Lee CH, Yang R, Petasis NA, Serhan CN. Resolvin D1 binds human phagocytes with evidence for proresolving receptors. *Proc Natl Acad Sci USA* 2010;107(4):1660–1665.
- [40]. LaMotte RH, Dong X, Ringkamp M. Sensory neurons and circuits mediating itch. *Nat Rev Neurosci* 2014;15(1):19–31. [PubMed: 24356071]
- [41]. LaMotte RH, Dong X, Ringkamp M. Sensory neurons and circuits mediating itch. *Nat Rev Neurosci* 2014;15(1):19–31.
- [42]. Latremoliere A, Woolf CJ. Central sensitization: a generator of pain hypersensitivity by central neural plasticity. *J Pain* 2009;10(9):895–926. [PubMed: 19712899]
- [43]. Lee SH, Tonello R, Im ST, Jeon H, Park J, Ford Z, Davidson S, Kim YH, Park CK, Berta T. Resolvin D3 controls mouse and human TRPV1-positive neurons and preclinical progression of psoriasis. *Theranostics* 2020;10(26):12111–12126. [PubMed: 33204332]
- [44]. Liu MZ, Chen XJ, Liang TY, Li Q, Wang M, Zhang XY, Li YZ, Sun Q, Sun YG. Synaptic control of spinal GRPR(+) neurons by local and long-range inhibitory inputs. *Proc Natl Acad Sci U S A* 2019.
- [45]. Liu Q, Tang Z, Surdenikova L, Kim S, Patel KN, Kim A, Ru F, Guan Y, Weng HJ, Geng Y, Undem BJ, Kollarik M, Chen ZF, Anderson DJ, Dong X. Sensory Neuron-Specific GPCR Mrgprs Are Itch Receptors Mediating Chloroquine-Induced Pruritus. *Cell* 2009.
- [46]. Liu R, Wang J, Chen Y, Collier JM, Capuk O, Jin S, Sun M, Mondal SK, Whiteside TL, Stolz DB, Yang Y, Begum G. NOX activation in reactive astrocytes regulates astrocytic LCN2 expression and neurodegeneration. *Cell Death Dis* 2022;13(4):371. [PubMed: 35440572]
- [47]. Liu T, Han Q, Chen G, Huang Y, Zhao LX, Berta T, Gao YJ, Ji RR. Toll-like receptor 4 contributes to chronic itch, allodynia, and spinal astrocyte activation in male mice. *Pain* 2016;157(4):806–817. [PubMed: 26645545]
- [48]. Liu T, Han Q, Chen G, Huang Y, Zhao LX, Berta T, Gao YJ, Ji RR. Toll-like receptor 4 contributes to chronic itch, allodynia, and spinal astrocyte activation in male mice. *Pain* 2016;157(4):806–817. [PubMed: 26645545]
- [49]. Liu T, Ji RR. New insights into the mechanisms of itch: are pain and itch controlled by distinct mechanisms? *Pflugers Arch* 2013;465(12):1671–1685. [PubMed: 23636773]
- [50]. Liu T, Ji RR. New insights into the mechanisms of itch: are pain and itch controlled by distinct mechanisms? *Pflugers Arch* 2013.
- [51]. Liu T, Xu ZZ, Park CK, Berta T, Ji RR. Toll-like receptor 7 mediates pruritus. *Nat Neurosci* 2010;13(12):1460–1462. [PubMed: 21037581]

- [52]. Liu XY, Liu ZC, Sun YG, Ross M, Kim S, Tsai FF, Li QF, Jeffry J, Kim JY, Loh HH, Chen ZF. Unidirectional cross-activation of GRPR by MOR1D uncouples itch and analgesia induced by opioids. *Cell* 2011;147(2):447–458. [PubMed: 22000021]
- [53]. Liu Y, Liu Y, Limjunyawong N, Narang C, Jamaldeen H, Yu S, Patiram S, Nie H, Caterina MJ, Dong X, Qu L. Sensory neuron expressed TRPC3 mediates acute and chronic itch. *Pain* 2022.
- [54]. Lukiw WJ, Cui JG, Marcheselli VL, Bodker M, Botkjaer A, Gotlinger K, Serhan CN, Bazan NG. A role for docosahexaenoic acid-derived neuroprotectin D1 in neural cell survival and Alzheimer disease. *J Clin Invest* 2005;115(10):2774–2783.
- [55]. Luo J, Feng J, Yu G, Yang P, Mack MR, Du J, Yu W, Qian A, Zhang Y, Liu S, Yin S, Xu A, Cheng J, Liu Q, O'Neil RG, Xia Y, Ma L, Carlton SM, Kim BS, Renner K, Liu Q, Hu H. Transient receptor potential vanilloid 4-expressing macrophages and keratinocytes contribute differentially to allergic and nonallergic chronic itch. *J Allergy Clin Immunol* 2018;141(2):608–619 e607. [PubMed: 28807414]
- [56]. Meixiong J, Vasavda C, Snyder SH, Dong X. MRGPRX4 is a G protein-coupled receptor activated by bile acids that may contribute to cholestatic pruritus. *Proc Natl Acad Sci U S A* 2019;116(21):10525–10530. [PubMed: 31068464]
- [57]. Moore C, Gupta R, Jordt SE, Chen Y, Liedtke WB. Regulation of Pain and Itch by TRP Channels. *Neurosci Bull* 2018;34(1):120–142. [PubMed: 29282613]
- [58]. Mrowietz U, Chouela EN, Mallbris L, Stefanidis D, Marino V, Pedersen R, Boggs RL. Pruritus and quality of life in moderate-to-severe plaque psoriasis: post hoc explorative analysis from the PRISTINE study. *J Eur Acad Dermatol Venereol* 2015;29(6):1114–1120. [PubMed: 25376448]
- [59]. Nesman JI, Chen O, Luo X, Ji RR, Serhan CN, Hansen TV. A new synthetic protectin D1 analog 3-oxa-PD1n-3 DPA reduces neuropathic pain and chronic itch in mice. *Org Biomol Chem* 2021;19(12):2744–2752. [PubMed: 33687402]
- [60]. Nguyen E, Lim G, Ding H, Hachisuka J, Ko MC, Ross SE. Morphine acts on spinal dynorphin neurons to cause itch through disinhibition. *Sci Transl Med* 2021;13(579).
- [61]. Park CK, Lu N, Xu ZZ, Liu T, Serhan CN, Ji RR. Resolving TRPV1- and TNF- α -mediated spinal cord synaptic plasticity and inflammatory pain with neuroprotectin D1. *J Neurosci* 2011;31(42):15072–15085. [PubMed: 22016541]
- [62]. Park CK, Xu ZZ, Liu T, Lu N, Serhan CN, Ji RR. Resolvin d2 is a potent endogenous inhibitor for transient receptor potential subtype v1/a1, inflammatory pain, and spinal cord synaptic plasticity in mice: distinct roles of resolvin d1, d2, and e1. *J Neurosci* 2011;31(50):18433–18438. [PubMed: 22171045]
- [63]. Patapoutian A, Tate S, Woolf CJ. Transient receptor potential channels: targeting pain at the source. *Nat Rev Drug Discov* 2009;8(1):55–68.
- [64]. Ralfkiaer U, Hagedorn PH, Bangsgaard N, Lovendorf MB, Ahler CB, Svensson L, Kopp KL, Vennegaard MT, Lauenborg B, Zibert JR, Krejsgaard T, Bonefeld CM, Sokilde R, Gjerdrum LM, Labuda T, Mathiesen AM, Gronbaek K, Wasik MA, Sokolowska-Wojdylo M, Queille-Roussel C, Gniadecki R, Ralfkiaer E, Geisler C, Litman T, Woetmann A, Glue C, Ropke MA, Skov L, Odum N. Diagnostic microRNA profiling in cutaneous T-cell lymphoma (CTCL). *Blood* 2011;118(22):5891–5900. [PubMed: 21865341]
- [65]. Ralvenius WT, Neumann E, Pagani M, Acuna MA, Wildner H, Benke D, Fischer N, Rostaher A, Schwager S, Detmar M, Frauenknecht K, Aguzzi A, Hubbs JL, Rudolph U, Favrot C, Zeilhofer HU. Itch suppression in mice and dogs by modulation of spinal alpha2 and alpha3GABAA receptors. *Nat Commun* 2018;9(1):3230. [PubMed: 30104684]
- [66]. Ross SE, Mardinly AR, McCord AE, Zurawski J, Cohen S, Jung C, Hu L, Mok SI, Shah A, Savner EM, Tolia C, Corfas R, Chen S, Inquimbert P, Xu Y, McInnes RR, Rice FL, Corfas G, Ma Q, Woolf CJ, Greenberg ME. Loss of inhibitory interneurons in the dorsal spinal cord and elevated itch in Bhlhb5 mutant mice. *Neuron* 2010;65(6):886–898. [PubMed: 20346763]
- [67]. Rowe B, Yosipovitch G. Malignancy-associated pruritus. *Eur J Pain* 2016;20(1):19–23. [PubMed: 26416212]
- [68]. Sanders KM, Akiyama T. The vicious cycle of itch and anxiety. *Neurosci Biobehav Rev* 2018;87:17–26. [PubMed: 29374516]

- [69]. Sawada Y, Honda T, Nakamizo S, Otsuka A, Ogawa N, Kobayashi Y, Nakamura M, Kabashima K. Resolvin E1 attenuates murine psoriatic dermatitis. *Sci Rep* 2018;8(1):11873. [PubMed: 30089836]
- [70]. Serhan CN. Pro-resolving lipid mediators are leads for resolution physiology. *Nature* 2014;510(7503):92–101. [PubMed: 24899309]
- [71]. Serhan CN, Dalli J, Karamnov S, Choi A, Park CK, Xu ZZ, Ji RR, Zhu M, Petasis NA. Macrophage proresolving mediator maresin 1 stimulates tissue regeneration and controls pain. *FASEB J* 2012;26(4):1755–1765. [PubMed: 22253477]
- [72]. Serhan CN, Hong S, Gronert K, Colgan SP, Devchand PR, Mirick G, Moussignac RL. Resolvins: a family of bioactive products of omega-3 fatty acid transformation circuits initiated by aspirin treatment that counter proinflammation signals. *JExpMed* 2002;196(8):1025–1037.
- [73]. Shiratori-Hayashi M, Koga K, Tozaki-Saitoh H, Kohro Y, Toyonaga H, Yamaguchi C, Hasegawa A, Nakahara T, Hachisuka J, Akira S, Okano H, Furue M, Inoue K, Tsuda M. STAT3-dependent reactive astrogliosis in the spinal dorsal horn underlies chronic itch. *NatMed* 2015;21(8):927–931.
- [74]. Shiratori-Hayashi M, Koga K, Tozaki-Saitoh H, Kohro Y, Toyonaga H, Yamaguchi C, Hasegawa A, Nakahara T, Hachisuka J, Akira S, Okano H, Furue M, Inoue K, Tsuda M. STAT3-dependent reactive astrogliosis in the spinal dorsal horn underlies chronic itch. *Nat Med* 2015;21(8):927–931. [PubMed: 26193341]
- [75]. Steinhoff M, Bienenstock J, Schmelz M, Maurer M, Wei E, Biro T. Neurophysiological, neuroimmunological, and neuroendocrine basis of pruritus. *JInvest Dermatol* 2006;126(8):1705–1718. [PubMed: 16845410]
- [76]. Sun YG, Chen ZF. A gastrin-releasing peptide receptor mediates the itch sensation in the spinal cord. *Nature* 2007;448(7154):700–703. [PubMed: 17653196]
- [77]. Sun YG, Zhao ZQ, Meng XL, Yin J, Liu XY, Chen ZF. Cellular basis of itch sensation. *Science* 2009;325(5947):1531–1534. [PubMed: 19661382]
- [78]. Terrando N, Gomez-Galan M, Yang T, Carlstrom M, Gustavsson D, Harding RE, Lindskog M, Eriksson LI. Aspirin-triggered resolvin D1 prevents surgery-induced cognitive decline. *FASEB J* 2013;27(9):3564–3571. [PubMed: 23709617]
- [79]. Tey HL, Yosipovitch G. Targeted treatment of pruritus: a look into the future. *Br J Dermatol* 2011;165(1):5–17. [PubMed: 21219293]
- [80]. Todd AJ. Neuronal circuitry for pain processing in the dorsal horn. *NatRevNeurosci* 2010;11(12):823–836.
- [81]. Tong F, He Q, Du WJ, Yang H, Du D, Pu S, Han Q. Sympathetic Nerve Mediated Spinal Glia Activation Underlies Itch in a Cutaneous T-Cell Lymphoma Model. *Neurosci Bull* 2022;38(4):435–439. [PubMed: 34870787]
- [82]. Tsuda M. Modulation of Pain and Itch by Spinal Glia. *Neurosci Bull* 2018;34(1):178–185. [PubMed: 28389872]
- [83]. Tungen JE, Aursnes M, Ramon S, Colas RA, Serhan CN, Olberg DE, Nuruddin S, Willoch F, Hansen TV. Synthesis of protectin D1 analogs: novel pro-resolution and radiotracer agents. *Org Biomol Chem* 2018;16(36):6818–6823. [PubMed: 30204204]
- [84]. van der Fits L, Mourits S, Voerman JS, Kant M, Boon L, Laman JD, Cornelissen F, Mus AM, Florencia E, Prens EP, Lubberts E. Imiquimod-induced psoriasis-like skin inflammation in mice is mediated via the IL-23/IL-17 axis. *J Immunol* 2009;182(9):5836–5845. [PubMed: 19380832]
- [85]. Wan T, Zhu W, Zhao Y, Zhang X, Ye R, Zuo M, Xu P, Huang Z, Zhang C, Xie Y, Liu X. Astrocytic phagocytosis contributes to demyelination after focal cortical ischemia in mice. *Nat Commun* 2022;13(1):1134. [PubMed: 35241660]
- [86]. Wang JC, Strichartz GR. Prevention of Chronic Post-Thoracotomy Pain in Rats By Intrathecal Resolvin D1 and D2: Effectiveness of Perioperative and Delayed Drug Delivery. *J Pain* 2017.
- [87]. Wang YH, Li Y, Wang JN, Zhao QX, Jin J, Wen S, Wang SC, Sun T. Maresin 1 Attenuates Radicular Pain Through the Inhibition of NLRP3 Inflammasome-Induced Pyroptosis via NF-kappaB Signaling. *Front Neurosci* 2020;14:831. [PubMed: 32982664]

- [88]. Wang Z, Jiang C, Yao H, Chen O, Rahman S, Gu Y, Zhao J, Huh Y, Ji RR. Central opioid receptors mediate morphine-induced itch and chronic itch via disinhibition. *Brain* 2021;144(2):665–681. [PubMed: 33367648]
- [89]. Wilson SR, Gerhold KA, Bifolck-Fisher A, Liu Q, Patel KN, Dong X, Bautista DM. TRPA1 is required for histamine-independent, Mas-related G protein-coupled receptor-mediated itch. *NatNeurosci* 2011;14(5):595–602.
- [90]. Wilson SR, Nelson AM, Batia L, Morita T, Estandian D, Owens DM, Lumpkin EA, Bautista DM. The ion channel TRPA1 is required for chronic itch. *J Neurosci* 2013;33(22):9283–9294. [PubMed: 23719797]
- [91]. Xu ZZ, Liu XJ, Berta T, Park CK, Lu N, Serhan CN, Ji RR. Neuroprotectin/protectin D1 protects against neuropathic pain in mice after nerve trauma. *Ann Neurol* 2013;74(3):490–495. [PubMed: 23686636]
- [92]. Xu ZZ, Zhang L, Liu T, Park JY, Berta T, Yang R, Serhan CN, Ji RR. Resolvins RvE1 and RvD1 attenuate inflammatory pain via central and peripheral actions. *NatMed* 2010;16(5):592–597, 591 p.
- [93]. Ye Y, Scheff NN, Bernabe D, Salvo E, Ono K, Liu C, Veeramachaneni R, Viet CT, Viet DT, Dolan JC, Schmidt BL. Anti-cancer and analgesic effects of resolvin D2 in oral squamous cell carcinoma. *Neuropharmacology* 2018;139:182–193. [PubMed: 30009833]
- [94]. Yosipovitch G Introduction for understanding and treating itch. *Dermatol Ther* 2013;26(2):83. [PubMed: 23551364]
- [95]. Yosipovitch G, Bernhard JD. Clinical practice. Chronic pruritus. *NEngJ Med* 2013;368(17):1625–1634.
- [96]. Yosipovitch G, Carstens E, McGlone F. Chronic itch and chronic pain: Analogous mechanisms. *Pain* 2007;131(1–2):4–7. [PubMed: 17524558]
- [97]. Yu H, Zhao T, Liu S, Wu Q, Johnson O, Wu Z, Zhuang Z, Shi Y, Peng L, He R, Yang Y, Sun J, Wang X, Xu H, Zeng Z, Zou P, Lei X, Luo W, Li Y. MRGPRX4 is a bile acid receptor for human cholestatic itch. *Elife* 2019;8.

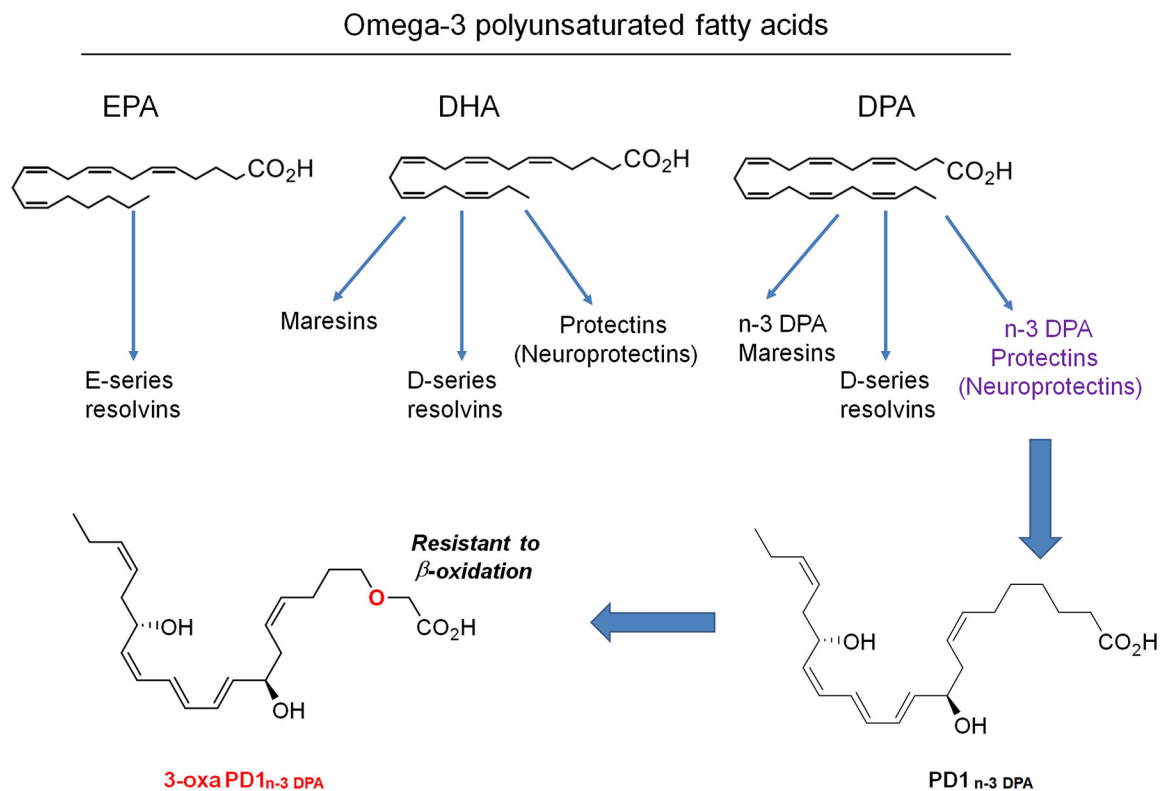


Fig. 1. Chemical structures of omega-3 polyunsaturated fatty acids EPA, DHA, and DPA, as well as n-3 DPA-derived PD1_{n-3} DPA and 3-oxa PD1_{n-3} DPA.

Note that 3-oxa PD1_{n-3} DPA is a synthetic compound and the 3-oxa insertion renders this lipid mediator resistant to β -oxidation metabolism.

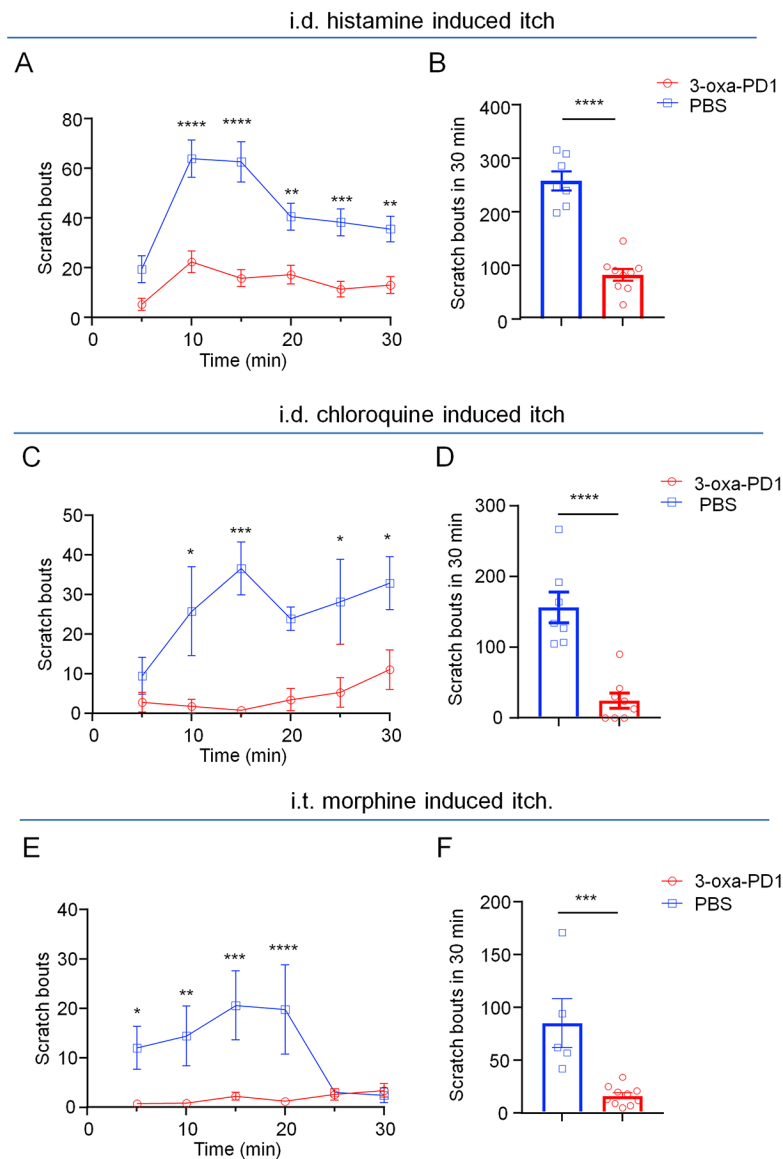


Figure 2. Intrathecal 3-oxa-PD1 inhibits acute itch.

Acute itch was evoked by intradermal injection of histamine (500 μ g, A-B), chloroquine (200 μ g C-D), and intrathecal administration of morphine (0.3 nmol, E-F). Intrathecal administration of 3-oxa-PD1 (100 ng), given 30 min prior to the injection of pruritogens, decreased the scratch bouts. (A, C, E) Time course of scratch bouts. Two-way ANOVA with Bonferroni's post hoc test. (A) $F_{(1, 14)} = 78.86$, $P < 0.0001$; (C) $F_{(1, 13)} = 31.69$, $P < 0.0001$; (E) $F_{(1, 13)} = 14.32$, $P = 0.023$. (B, D, F) Accumulating bouts in 30 min. Unpaired t-test. Vehicle (PBS): $n = 7$ (A), $n = 8$ (C), $n = 5$ (F); Oxa-PD1: $n = 9$ (A), $n = 8$ (C), and $n = 10$ (F). Data are shown as mean \pm SEM. * $P < 0.05$, ** $P < 0.01$, *** $P < 0.001$, **** $P < 0.0001$.

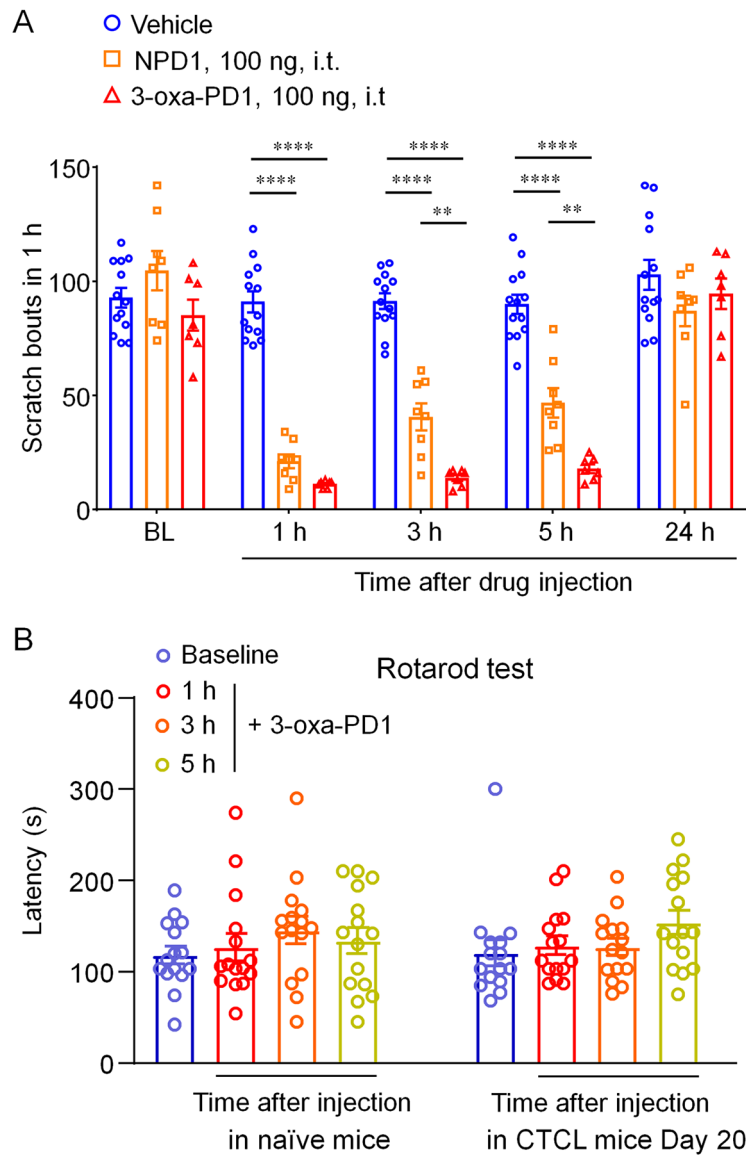


Figure 3. Effects of intrathecal 3-oxa-PD1 and NPD1 on CTCL-induced chronic itch and motor function.

(A) NPD1 and 3-oxa-PD1 (100 ng, i.t.) significantly reduced the number of scratches, compared to vehicle ($n = 13$), at 1, 3 and 5 hours. Compared with NPD1 ($n = 8$), 3-oxa-PD1 ($n = 7$) produced greater inhibition of scratching at 3 and 5 hours. Two-way ANOVA with Bonferroni's post hoc test. $F_{(2, 25)} = 120.8$, $P < 0.0001$. ** $P < 0.01$, **** $P < 0.0001$. (B) Rotarod testing showing the effects of 3-oxa-PD1 (100 ng, i.t.) on motor function in naïve animals and CTCL animals (Day 20). $n = 15$ mice per group. Note that fall latency is slightly increased after 3-oxa-PD1 treatment. Data are shown as mean \pm SEM.

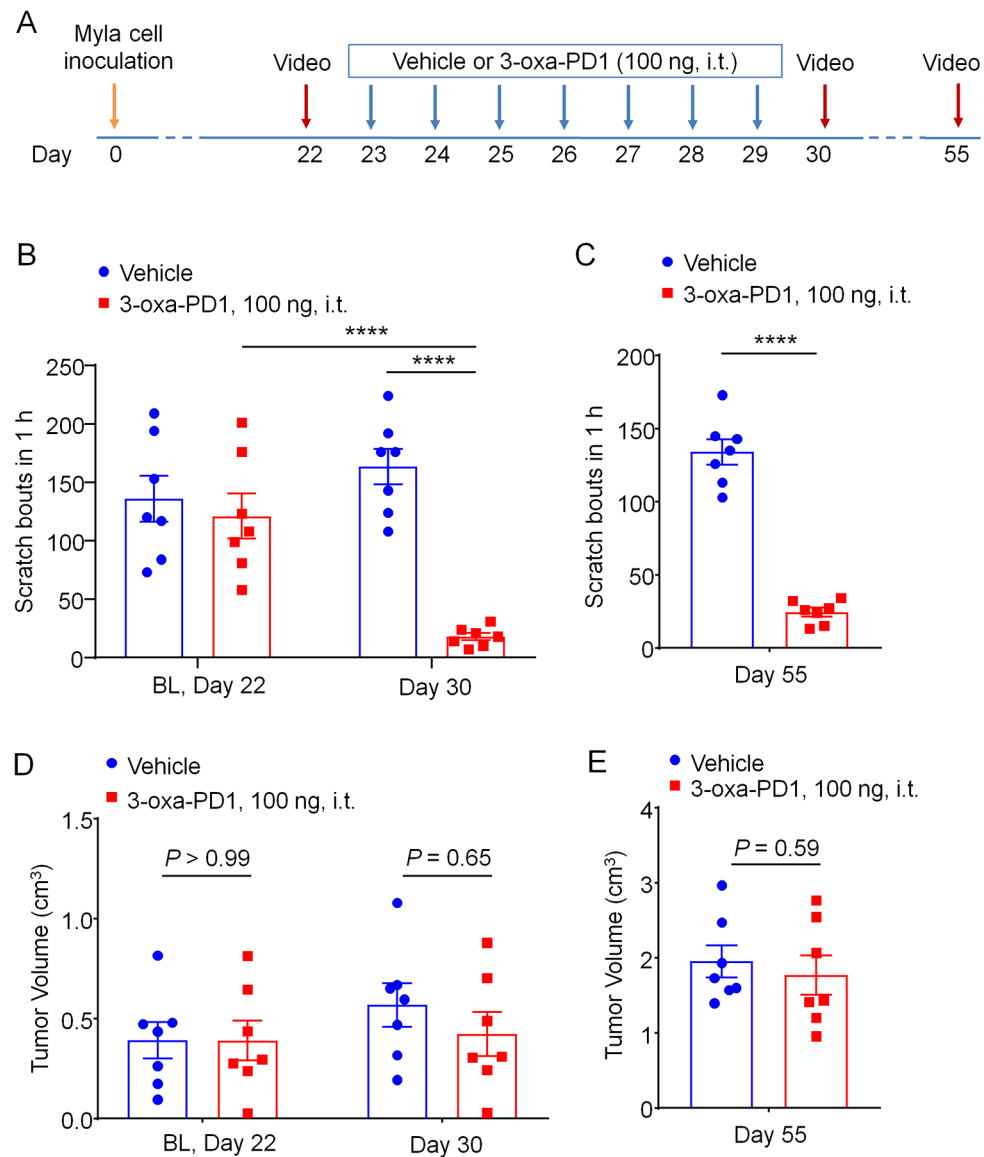


Figure 4. Effects of persistent intrathecal 3-oxa-PD1 treatment on chronic itch and tumor growth.

(A) Experimental paradigm of oxa-PD1 treatment and behavioral testing. Daily i.t. injection of 3-oxa-PD1 (100 ng) was given for 7 days, starting on CTCL day 23. Itching behavior was video recorded on Day 30 and Day 55. (B-C) Repeated i.t. administration of 3-oxa-PD1 substantially reduced the number of scratching in early-mid phase (Day 30, B) and late-phase (Day 55, C). $n = 7$ mice/group, Two-way ANOVA with Bonferroni's post hoc test. $F_{(1, 12)} = 17.54$, $P < 0.0013$ (B); unpaired t-test (C). (D-E) The same oxa-PD1 treatment did not affect the tumor growth in either early or late phase. $n = 7$ mice/group, Two-way ANOVA with Bonferroni's post hoc test. $F_{(1, 12)} = 0.2567$, $P = 0.62$ (D); unpaired t-test (E). Data are shown as mean \pm SEM. **** $P < 0.0001$.

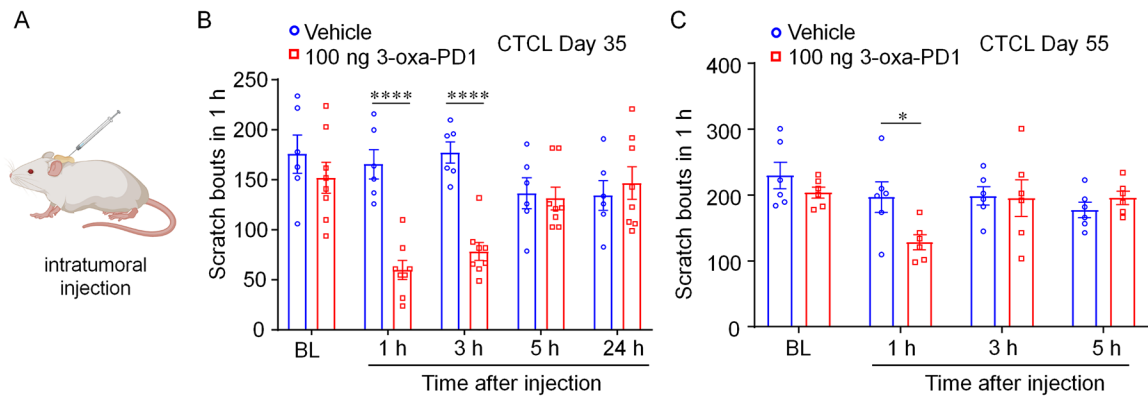


Figure 5: Intratumoral injection of 3-oxa-PD1 inhibits cancer itch.

(A) Schematic of intra-tumor injection. (B) Intra-tumor injection of 3-oxa-PD1 (100 ng, $n = 8$), given on CTCL Day 35, reduced itching behavior at 1 and 3 hours after administration. **** $P < 0.0001$, compared with vehicle ($n = 6$), Two-way ANOVA with Bonferroni's post hoc test. $F_{(1, 12)} = 10.04$, $P = 0.0081$. (C) Intra-tumor injection of 3-oxa-PD1 (100 ng, $n = 6$), given on CTCL Day 55, reduced itching behavior at 1 hour after administration. * $P < 0.05$, compared with vehicle ($n = 6$), Two-way ANOVA with Bonferroni's post hoc test. $F_{(1, 12)} = 10.04$, $P = 0.0081$. Data are shown as mean \pm SEM.

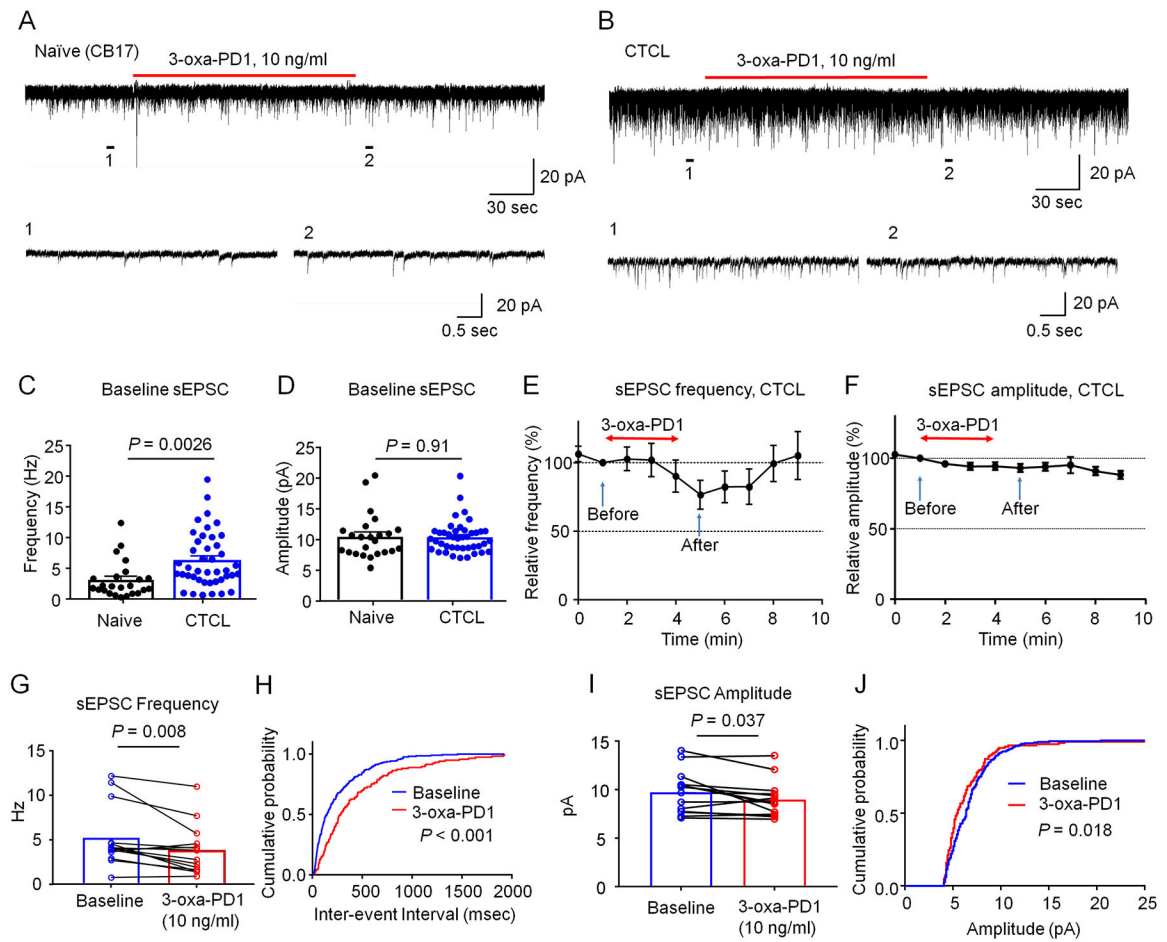


Figure 6. 3-oxa-PD1 inhibits excitatory synaptic transmissions in spinal cord slices of CTCL mice.

(A-B) Representative traces of spontaneous EPSCs (sEPSCs) in lamina IIo neurons of naïve CB17 (A) and CTCL (B) mice. Traces 1 and 2 are enlarged in the bottom panels. (C-D) Quantification of sEPSC frequency (C) and amplitude (D) in naïve and CTCL mice. CTCL significantly increased the frequency but not amplitude of sEPSC. Unpaired t-test, $n = 24$ neurons from 7 naïve mice and $n = 42$ neurons from 10 CTCL mice of both sexes. (E, F) Time course showing the effects of bath application of 3-oxa-PD1 (10 ng/ml, 3 min) on percentage changes of sEPSC frequency (E, $n=14$ neurons) and sEPSC amplitude (F, $n=14$ neurons). Arrows indicate before and after 3-oxa-PD1 perfusion. Note that 3-oxa-PD1 decreased the frequency but not amplitude of sEPSCs in spinal cord neurons of CTCL mice. Also note the effect of 3-oxa-PD1 can be washed out in 5 min. (G) sEPSC frequency. Paired t-test, $n = 14$ neurons from 5 CTCL mice. (H) Cumulative probability of inter-event interval shows longer interval after 3-oxa-PD1 application. Two-sample Kolmogorov-Smirnov test. (I) sEPSC amplitude. $n = 14$ neurons from 5 CTCL mice. (J) Cumulative probability of amplitude. The data were analyzed at 1 min (before treatment) and 5 min (after treatment). Data are shown as mean \pm SEM.

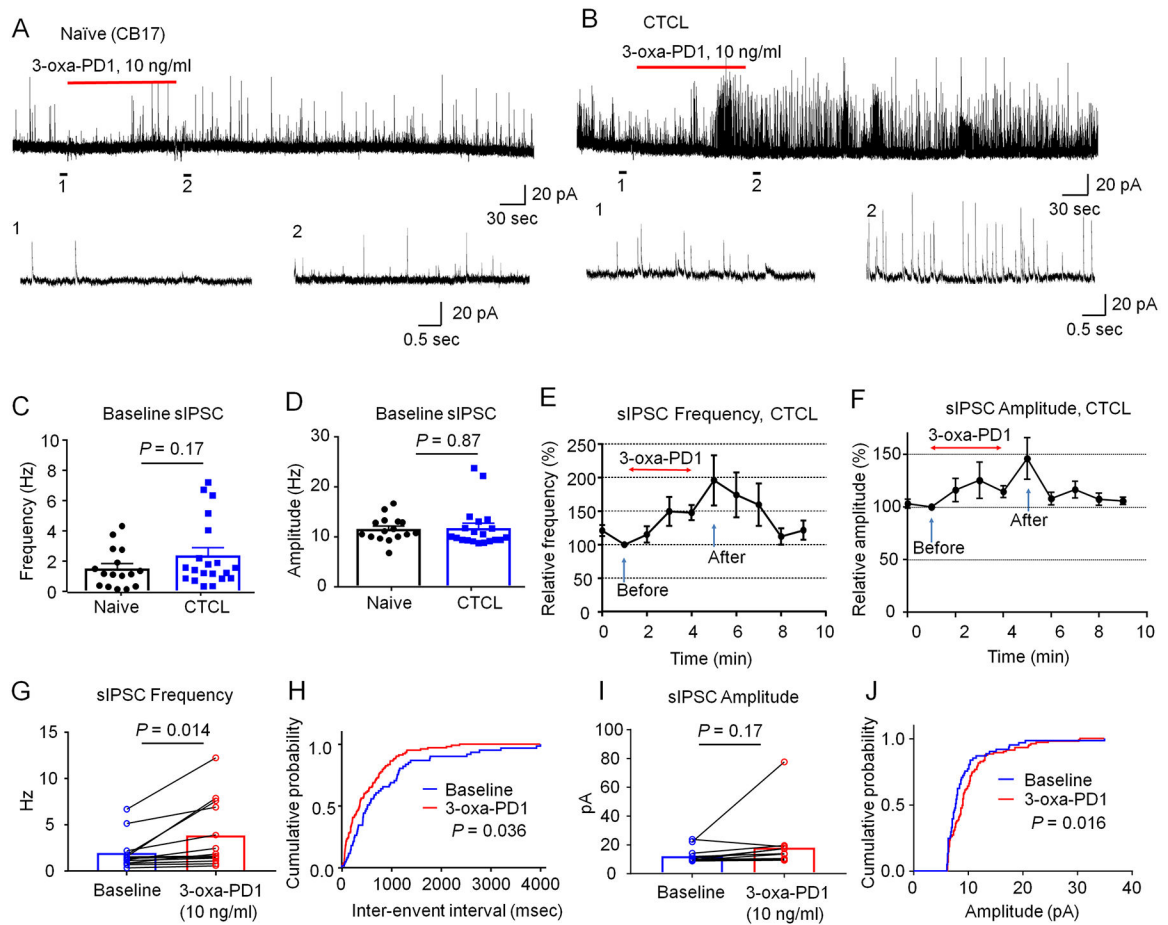


Figure 7. 3-oxa-PD1 increases inhibitory synaptic transmissions in spinal cord slices of CTCL mice.

(A-B) Representative traces of spontaneous IPSCs (sIPSC) in lamina IIo neurons of naïve CB17 (A) and CTCL (B) mice. Traces 1 and 2 are enlarged in the bottom panels. (C-D) Quantification of sIPSC frequency in naïve and CTCL mice. Unpaired t-test, $n = 16$ neurons from 4 naïve mice and $n = 20$ neurons from 3 CTCL mice of both sexes. (E, F) Time course showing the effects of bath application of 3-oxa-PD1 (10 ng/ml, 3 min) on percentage changes of sIPSC frequency (E, $n=13$ neurons) and sEPSC amplitude (F, $n=13$ neurons). Arrows indicate before and after 3-oxa-PD1 perfusion. Note that 3-oxa-PD1 decreased the frequency but not amplitude of sEPSCs in spinal cord neurons of CTCL mice. Also note the effect of 3-oxa-PD1 can be washed out in 5 min. (G) sIPSC frequency in CTCL mice. Paired t-test, $n = 13$ neurons from 3 CTCL mice. (H) Cumulative probability of inter-event interval shows shorter interval after Oxa-PD1 application. Two-sample Kolmogorov-Smirnov test. (I) sEPSC amplitude. Paired t-test, $n = 13$ neurons from 3 CTCL mice. (J) Cumulative probability of amplitude. The data were analyzed at 1 min (before treatment) and 5 min (after treatment). Data are shown as mean \pm SEM.

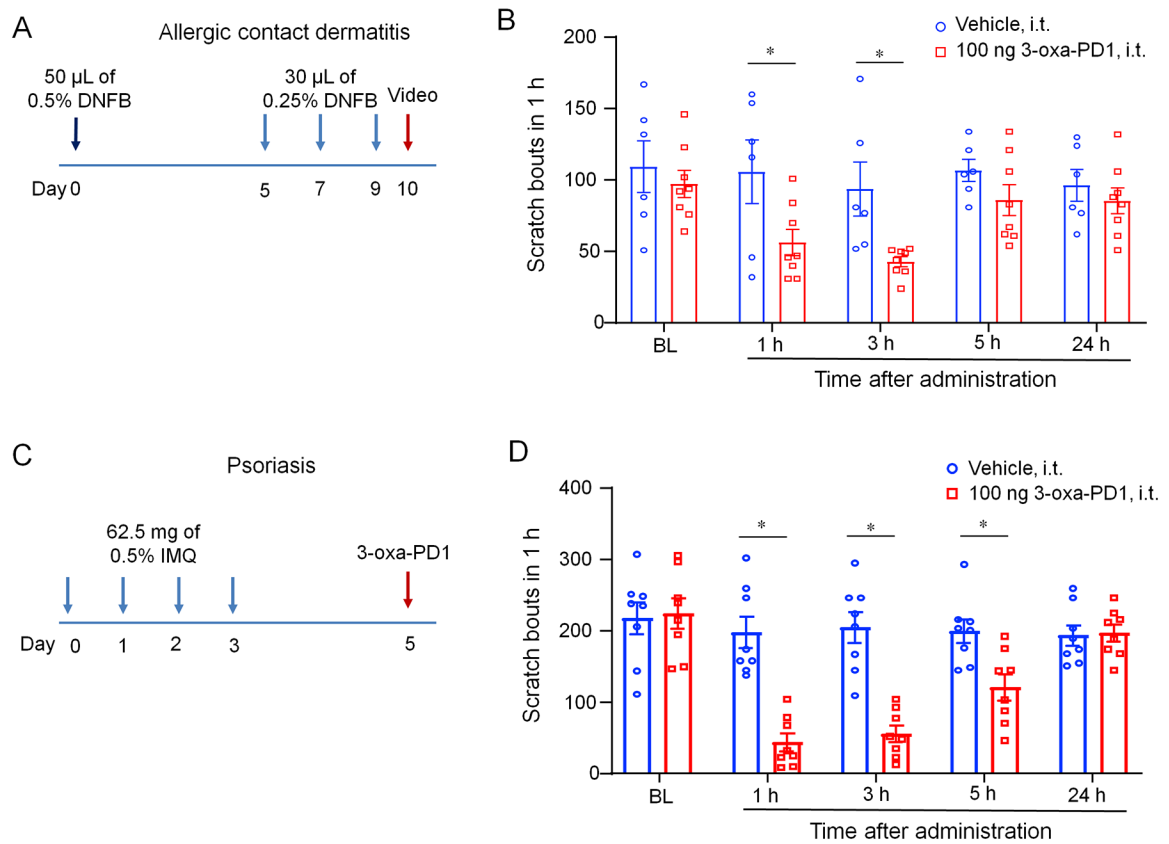


Figure 8. Intrathecal 3-oxa-PD1 treatment inhibits persistent itch in mice following DNFB-induced dermatitis and imiquimod-induced psoriasis.

(A) Protocol of experimental design for the mouse DNFB model. (B) Intrathecal administration of 3-oxa-PD1 (100 ng) reduced the number of scratching. Two-way ANOVA with Bonferroni's post hoc test. $F_{(1, 60)} = 13.68$, $n=6$ mice (vehicle) and $n=8$ mice (3-oxa-PD1). (C) Protocol of experimental design for the mouse psoriasis model induced by imiquimod (IMQ). (D) Intrathecal administration of 3-oxa-PD1 (100 ng) reduced the number of scratching. Two-way ANOVA with Bonferroni's post hoc test. $F_{(1, 60)} = 13.68$, $n=6$ mice (vehicle) and $n=8$ mice (3-oxa-PD1). Data are shown as mean \pm SEM. * $P < 0.05$,

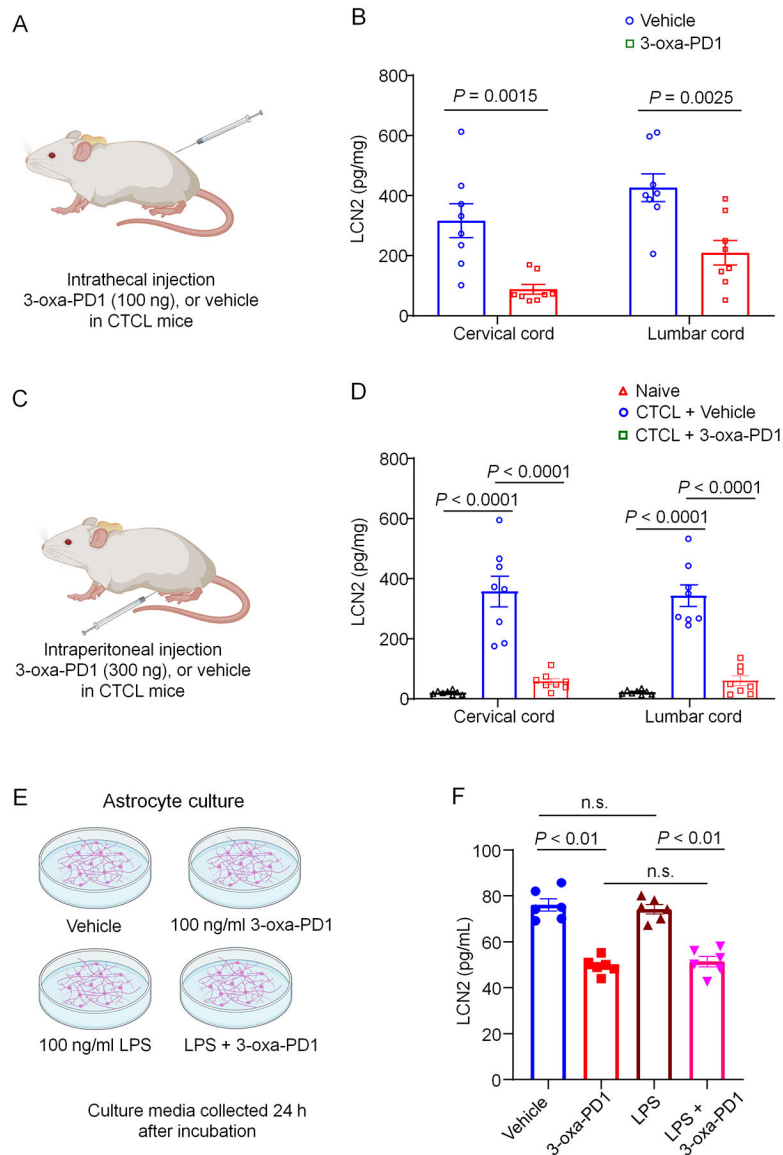


Figure 9: 3-oxa-PD1 inhibits spinal production of LCN2 production in CTCL mice and LCN2 secretion in astrocyte cultures.

(**A, B**) Intrathecal injection of 3-oxa-PD1 (100 ng, **A**) inhibited LCN2 production in cervical and lumbar segment of spinal cord in CTCL mice. Two-way ANOVA with Bonferroni's post hoc test. $F_{(1, 28)} = 27.17$, $P < 0.0001$. $n = 8$ per group. (**C, D**) Intraperitoneal injection of 3-oxa-PD1 (300 ng, **C**) inhibited LCN2 production in cervical and lumbar segment of spinal cord in CTCL mice. Note that LCN2 level is very low in naïve animals and substantially increased in CTCL mice. Two-way ANOVA with Bonferroni's post hoc test. $F_{(1, 28)} = 27.17$, $P < 0.0001$. Spinal cord tissues were collected 3 h after 3-oxa-PD1 administration on CTCL Day 45. $n = 8$ per group. (**E, F**) 3-oxa-PD1 treatment in primary cultures of astrocytes (**E**) inhibited LCN2 secretion in culture medium. One-way ANOVA with Bonferroni's post hoc test. $F_{(2, 42)} = 89.62$, $P < 0.0001$. $n = 6$ per group. LCN2 levels were measured by ELISA using commercial kits. Data are shown as mean \pm SEM.

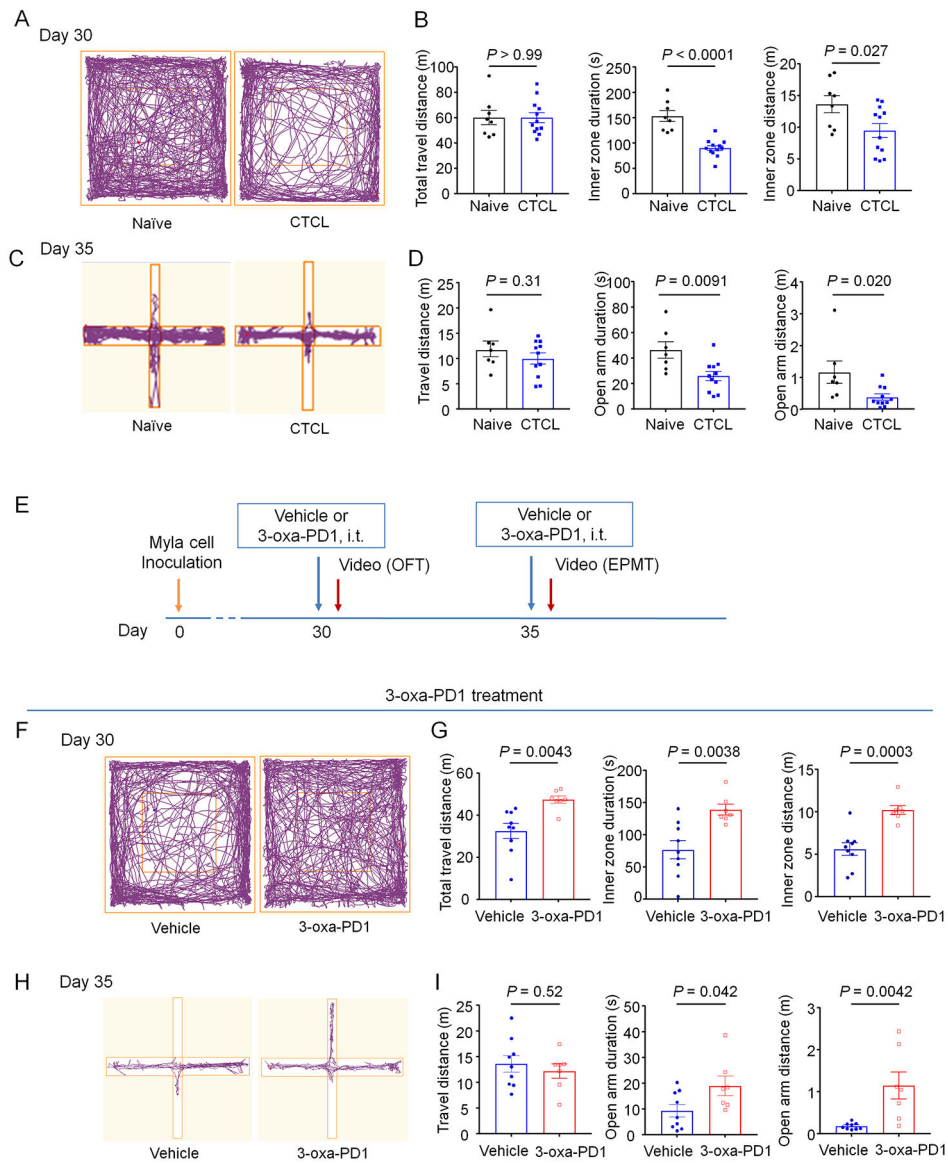


Figure 10. Intrathecal 3-oxa-PD1 treatment alleviates CTCL-induced anxiety in mice. Anxiety-related behavior was assessed by open field test (A-B, E-F) and elevated plus maze test (C-D, G-H). (A-B) CTCL mice show significantly shorter inner zone travel duration and distance than naïve mice. $n = 8$ (naïve) and $n = 12$ (CTCL). (C-D) CTCL mice show significantly shorter open arm duration and distance than naïve mice. $n = 7$ (naïve) and $n = 11$ (CTCL). (E) Schematic of experimental design for drug administration and behavioral testing. EPMT, elevated plus maze testing; OFT, open-field testing. (F-G) In CTCL model mice, intrathecal administration of Oxa-PD1 (100 ng) significantly increased the inner zone travel duration and distance in open-field test compared to vehicle group. $n = 9$ (vehicle) and $n = 7$ (3-oxa-PD1). (H-I) Both the travel duration and distance in open arm were significantly longer in 3-oxa-PD1 treated group than vehicle group. $n = 9$ (vehicle) and $n = 7$ (3-oxa-PD1). Data are shown as mean \pm SEM. Unpaired t-test (B, D, G, I).

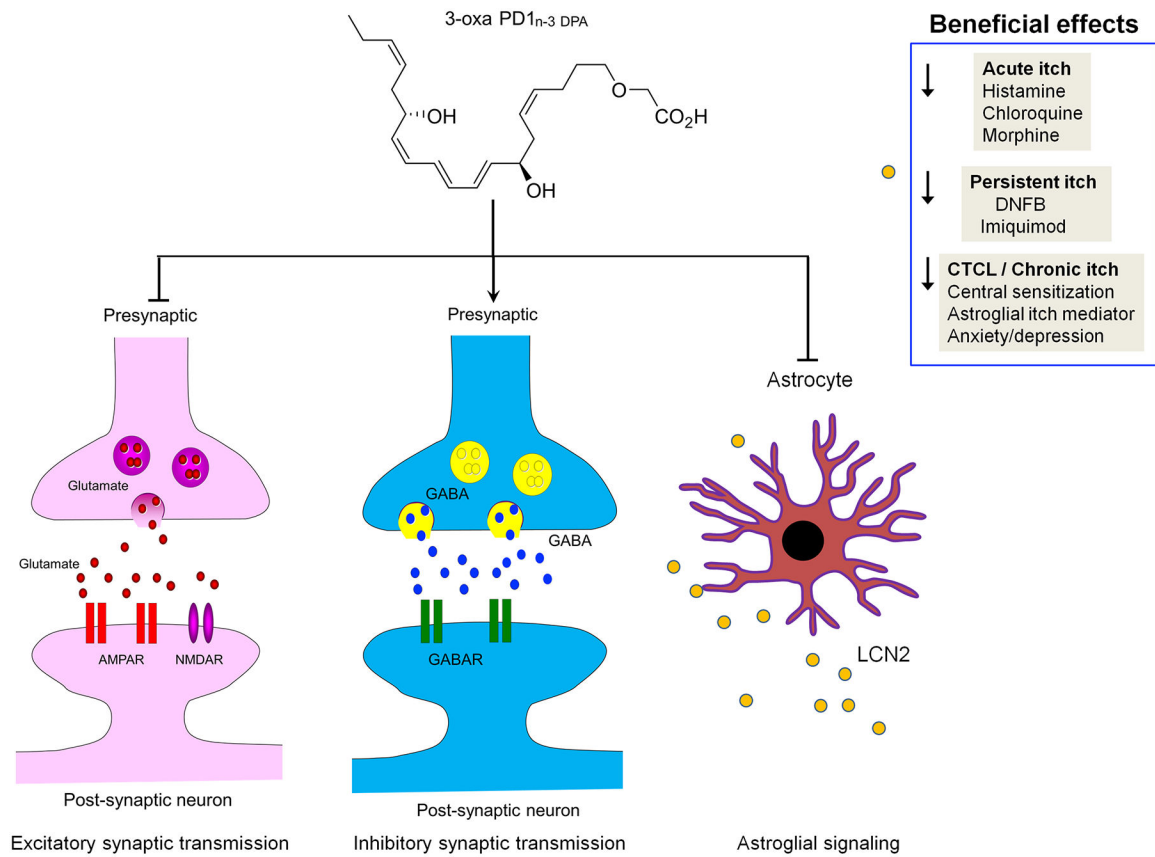


Figure 11. Schematic of multiple benefits of 3-oxa-PD1 and mechanism of action.

Local and systemic injection of 3-oxa-PD1 reduces acute, persistent, and chronic itch

in mouse models. 3-oxa-PD1 inhibits central sensitization in spinal cord neurons by modulation of both excitatory and inhibitory synaptic transmission in CTCL mice.

Furthermore, 3-oxa-PD1 can suppress spinal cord production and astrocyte release of LCN2, an astrocyte-produced itch mediator.